



## Vertical and horizontal variation of aerosol number size distribution in the boreal environment

Riikka Väänänen<sup>1</sup>, Radovan Krejci<sup>2,1</sup>, Hanna E. Manninen<sup>1</sup>, Antti Manninen<sup>1</sup>, Janne Lampilahti<sup>1</sup>, Stephany Buenrostro Mazon<sup>1</sup>, Tuomo Nieminen<sup>3,1</sup>, Taina Yli-Juuti<sup>3,1</sup>, Jenni Kontkanen<sup>1</sup>, Ari Asmi<sup>1</sup>, Pasi P. Aalto<sup>1</sup>, Petri Keronen<sup>1</sup>, Toivo Pohja<sup>1,4</sup>, Ewan O'Connor<sup>5</sup>, Veli-Matti Kerminen<sup>1</sup>, Tuukka Petäjä<sup>1</sup>, Markku Kulmala<sup>1</sup>

<sup>1</sup>Department of Physics, P.O. Box 64, FI-00014 University of Helsinki, Finland

<sup>2</sup>Stockholm University, Department of Environmental Science and Analytical Chemistry & Bolin Centre for Climate Research, SE-10691 Stockholm, Sweden

10 <sup>3</sup>Department of Applied Physics, University of Eastern Finland, P.O. Box 1627, FI-70211 Kuopio, Finland

<sup>4</sup>SMEAR II measurement station, Hyytiäläntie 124, 35500 Korkeakoski, Finland

<sup>5</sup>Finnish Meteorological Institute, P.O. BOX 503, FI-00101 Helsinki, Finland

Correspondence to: R. Väänänen ([riikka.vaananen@helsinki.fi](mailto:riikka.vaananen@helsinki.fi))

### 15 Abstract

This study explores the vertical and horizontal variability of the particle number size distribution from two flight measurements campaigns over a boreal forest in Hyytiälä, Finland during May–June 2013 and March–April 2014, respectively. Our other aims were to study the spatial extent of new particle formation events and to compare the airborne observation with the ground measurements from the SMEAR II (Station for Measuring Ecosystem-Atmosphere Relations) field station located in Hyytiälä. 20 The airborne measurements extended vertically 3.8 km and horizontally 30 km from the station. A Cessna 172 aircraft was used as a measurement platform. The measured parameters included the particle number concentration (>3 nm) and particle number size distribution (10–400 nm). The airborne data used in this study were equal to 111 flight hours. The measurements showed that despite local fluctuations there was a good agreement between the on-ground and airborne measurements inside the planetary boundary layer. On median, the airborne total number concentration was found to be 10 % larger than at the 25 ground level. The seasonal and meteorological differences between the campaigns were reflected in aerosol properties. NPF days showed areas of intensified NPF on a scale from kilometres up to couple of tens of kilometres in the planetary boundary layer. NPF was also observed frequently in the free troposphere.



## 1 Introduction

Atmospheric measurements performed at ground-based stations are often generalized to represent the conditions on the larger scale. However, the spatial and temporal scales of the complex atmospheric phenomena, like new particle formation (NPF), and information on spatial variability of aerosol properties is needed for correct extrapolation and parametrization of ground-based observations to larger scale and for use in modelling studies.

Numerous measurement have shown that the NPF from precursor gases (Kulmala et al. 2013, Kulmala et al. 2014) occurs frequently around the world (Kulmala and Kerminen 2008, Kulmala et al. 2004, Zhang et al. 2012), and that the subsequent growth of these fresh-born particles is a climatically important source of cloud condensation nuclei (CCN) (Kerminen et al. 2012). Model studies by Spracklen et al (2008) and Merikanto et al (2009) show that NPF in the planetary boundary layer (PBL) can increase the global PBL CCN production up to 50 %. The Hyytiälä SMEAR II (Station for Measuring Ecosystem-Atmosphere Relations) measurement site located in Southern Finland has provided an extensive two-decade long measurement time series of aerosol properties in a rural boreal forest environment (Hari and Kulmala 2005, Nieminen et al. 2014). In Hyytiälä, NPF days are occurring regularly on around 25% of the days with a peak observed during the spring when NPF occurs almost every other day on average (Dal Maso et al. 2005, Nieminen et al. 2014).

Although temporary limited to field campaigns of various lengths typically on scale of weeks, airborne measurements add important information about the spatial variability of the parameters of interest. Only few long-term data sets exist. The European Research Infrastructure IAGOS has used commercial passenger aircrafts to obtain a 20-year data set of atmospheric components in the troposphere and stratosphere with global spatial coverage (Petzold et al. 2015). Two extensive studies to characterize the vertical profiles of aerosol optical parameters were performed over Oklahoma (Andrews et al. 2011) and over Illinois (Sheridan et al. 2012).

As part of the EUCAARI campaign (Kerminen et al. 2010, Kulmala et al. 2011) airborne aerosol observations were performed over Europe. Hamburger et al (2011) compared the data from several European measurement stations to airborne accumulation mode particles inside the PBL with a maximum distance of 150 km from the selected station. They found a good agreement between the airborne and ground measurements. During the same campaign, the horizontal scale of the NPF was determined on a scale up to 100 km, and the NPF was observed only inside the PBL (Crume rolle et al. 2010).

Within EUCAARI, the vertical extent of NPF was studied with a helicopter-borne platform in Cabauw, Netherlands (Wehner et al. 2010), and it was found that NPF started in a turbulent layer above the convective boundary layer before NPF was observed at ground. This was observed also in later campaigns with unmanned aircraft systems (UASs) in Melpliz, Germany. It was explained that whereas the mean values of the meteorological parameters and the saturation vapour pressures of the needed condensable vapours were not favourable enough for nucleation, the turbulence in these layers could create pockets where nucleation was able to start. This process was proposed already earlier by Nilsson et al (2001). Also, at the top of the



boundary layer with lower ambient temperature conditions for NPF are thermodynamically more favourable than the ones at the ground level (Easter and Peters 1994).

In Hyytiälä, there have been several studies on the vertical extent of the NPF process. O'Dowd et al (2009) conducted measurements with small and microlight aircrafts. Nucleation mode particles peaked first at the lowest altitudes, just above the canopy top. Laakso et al (2007) examined the vertical profiles of NPF with an instrumented hot-air balloon and found that the NPF started simultaneously at all altitudes in the PBL. However, the results of Schobesberger et al (2013) indicate that NPF was enhanced in the upper part of the PBL.

The airborne measurements inside the PBL with longer horizontal constant-altitude legs have revealed horizontal variability in the ultrafine aerosol concentrations during NPF (Crumeyroille et al. 2010, O'Dowd et al. 2007, O'Dowd et al. 2009, Schobesberger et al. 2013). However, to our knowledge, this variation has not been quantified using larger data set. The horizontal variation has been studied by simultaneous measurements at two or more closely located stations (e.g. Komppula et al. 2003, Wehner et al. 2007) but this approach lacks the spatially continuous row of measurement points and thus the full extent of the NPF cannot be revealed.

Several studies have previously reported nucleation also in the free troposphere (FT). Laakso et al. (2007) and Schobesberger et al. (2013) reported single measurements of nucleation mode particles in the FT above Hyytiälä. During a two-month campaign over the Mediterranean, Rose et al. (2015) observed regularly 5–10 nm particles in the FT, also during nights. Their study showed that due to the low condensation sink at altitudes between 2000–3000 m there had been favourable conditions for NPF. Mirme et al (2010) measured in the FT up to the altitudes over 10 km, and reported both neutral and charged sub-3 nm clusters at all altitudes. The results from a five-year measurements in continental FT over Siberia by Paris et al (2009) showed that the ratio of concentrations of 3–70 nm and 70–200 nm particles ( $N_{3-70}/N_{70-200}$ ) was higher over 5 km than below it. In recent measurements at Jungfraujoch research station (3580 m a.s.l), Switzerland, NPF was observed on 15–20 % of the days, and the air mass had lifted the condensable vapours from PBL 1–2 day before the NPF was observed in the FT (Bianchi et al. 2016).

This paper presents the results from two airborne campaigns in May–June 2013 and in March–April 2014 during clearly different meteorological conditions. Both campaigns provide rather extensive data sets on the vertical and horizontal variability of aerosol number size distribution in the boreal environment. The spring seasons were chosen since it is when NPF is most frequent in Hyytiälä. The main goals of this study were 1) to characterize the vertical aerosol distribution and its variation in the PBL and the lowermost free troposphere, 2) to compare airborne measurements on horizontal scale of tens of kilometres with the ground based observations, 3) to study the spatial extent of NPF both in the PBL and free troposphere, 4) to investigate the night-time residual layer after a NPF day.



## 2 Methods

### 2.1 Airborne instrumentation and data preparation

We used a Cessna 172 aircraft as a measurement platform (Schobesberger et al. 2013) (Fig. 1). The Cessna 172 is a four-seat single engine airplane. Its payload is limited by size and weight. An advantage is its low cruising speed, around 35 m/s, and relatively low infrastructure and running costs.

The forward facing sample air inlet was mounted under the right wing. It is a modified version of the shrouded inlet used by Hawaii University on board of NASA DC-8 aircraft (McNaughton et al. 2007). The sample air was taken through a 4.2-meters and 22-mm diameter stainless steel tube into the cabin. The scientific operator used a manual control of a Venturi tube to keep the sample flow at  $50 \text{ l min}^{-1}$ . This ensured that the pressure of the instrument inlets was equal to the outside pressure, and the sampling was conducted close to isokinetic conditions.

The aerosol and gas instruments were in a rack situated in the cabin. The air for individual instruments was sampled using core inlets, i.e. from the centre of the main flow. An ultrafine Condensation Particle Counter (uCPC, Model 3776, TSI Inc.) was used to measure the number concentration of particles larger than 3 nm. The aerosol number size distribution in the size range of 10–400 nm was measured using a custom-made Scanning Mobility Particle Sizer (SMPS) with a short Hauke type Differential Mobility Analyzer (DMA) operating with closed-loop sheath air and a TSI 3010 CPC as a particle counter. A Li-Cor Li-840 analyzer was used to measure  $\text{H}_2\text{O}$  and  $\text{CO}_2$  mixing ratios (MRs). A Particle Size Magnifier (PSM, Model A09, Airmodus, Vanhanen et al. 2011) connected to a TSI 3772 CPC was tested and optimized for the observations of newly formed aerosol particles as small as 1.5 nm. Finally, an Optical Particle Sizer (OPS, Model 3330, TSI Inc.) was used during some flights in 2014 to measure the particles with sizes larger than 300 nm. The sample flows of the instruments were maintained either by internal pumps of the instruments or by an external pump. Accumulators provided electricity for the instruments.

Aerosol and gas measurements were complemented by the basic meteorological parameters. A fast PT-100 temperature sensor was mounted under the wing inside a metallic housing with free flow of passing air. A relative humidity sensor and a second temperature sensor were located under the inlet inside a metal housing. Static air pressure was measured inside the unpressurized cabin. A GPS receiver recorded the 3D position of the aircraft.

The particle and gas instruments were tested and calibrated in the laboratory before the airborne measurements. The CPCs were calibrated against a reference electrometer. A reference DMA was used to determine both the cut-off sizes of the CPCs and the sizing accuracy of the SMPS. The Li-Cor 840 was calibrated using standard gases for  $\text{CO}_2$  and  $\text{H}_2\text{O}$ .

All aerosol data reported in this study were corrected to the standard temperature and pressure (STP, 100 kPa and 273.15 K) conditions. The SMPS data were inverted using the schema by Collins et al (2002). All the data, except the particle size distributions measured with the SMPS were recorded at 1 Hz. The SMPS had two-minute resolution. For the analysis involving aerosol size distribution, 2 min mean values of other quantities were calculated from the 1 Hz data. After the PEGASOS 2013



campaign, we performed a 2-day side-by-side comparison between the aircraft SMPS and CPC, and the ground-based DMPS at Hyytiälä. The total particle concentrations measured at Hyytiälä differed from those measured by the Cessna uCPC and SMPS less than 10 %. The mode peak diameters measured by the Hyytiälä DMPS showed typically 1–2 nm larger particles than those measured by Cessna SMPS.

## 5 2.2 Flight campaigns and their meteorological characteristics

The most favourable season for the NPF events at the SMEAR II station is spring (Dal Maso et al. 2008, Nieminen et al. 2014). Meteorological conditions during March–April in 2014 and May–June in 2013 differed clearly from each other, and therefore we present them separately, and refer to them as ‘late spring 2013’, and ‘early spring 2014’. The origin of the air masses during the measurement campaigns was determined using the HYSPLIT trajectory analysis (Rolph 2016, Stein et al. 2015). The satellite images by the NOAA-satellites carrying AVHRR sensors were used to determine the cloud cover along the trajectory of the air masses (<http://www.sat.dundee.ac.uk>). The thermal infra-red channel (10.3–11.3 $\mu$ m) was used.

The planetary boundary layer (PBL), which is the lowermost and well-mixed atmospheric layer directly connected to the surface, develops and rises during the morning (Stull 2012). Within the mixed PBL the potential temperature and H<sub>2</sub>O MR are relative constant (Stull 2012), and we used their airborne calculated vertical profiles to determine the height of the PBL. During the campaigns reported in this paper, the daily maximum height of the PBL varied between 0.6 km and 2.5 km.

During the late spring 2013, there was a warm three-week period between 16 May and 6 June when air masses originated from east and the daily maximum temperatures often exceed 20 °C. Before and after this period the air masses arrived from westerly directions and daily temperatures were around 15 °C or lower (Nieminen et al. 2015).

The early spring campaign 2014 started with a 6-day period with the daily maximum temperatures varying between 5 and 9 °C. This was followed by a 6-day period with the daily maximum temperatures between –1 and 3 °C. During the last week of the campaign, the daily temperatures were around 3–4 °C. The prevailing origin of the air masses were Atlantic Ocean or Arctic Ocean: the only flights days in air masses of non-marine origins were carried out on 25 March and 2 April 2014.

Western and northern air masses advected to Hyytiälä from Atlantic and Arctic Oceans are typically cleaner than the southern or eastern air masses, which originate from continental and more populated regions (Nieminen et al. 2014, Sogacheva et al. 2005).

## 2.3 Flight strategy

The airborne measurements were part of larger field campaigns focused on biosphere-atmosphere interactions in a boreal forest environment. During the PEGASOS Northern Mission in 2013, Cessna observations were carried out in coordinated manner with Zeppelin NT airship measurements (Manninen et al, in preparation), and an extensive field campaign was performed at the SMEAR II station. During 2014, the BA ECC campaign was a joint project between University of Helsinki and the U.S.



Department of Energy's ARM Mobile Facility (Petäjä et al. 2016). A three-week flight campaign in March–April was part of one of the BA ECC campaign's three Intensive Operational Period (IOP).

During the late spring 2013 flight campaign, a total of 45 measurement flights were flown in 30 days between 24 April and 15 June 2013. During the early spring 2014 campaign, 26 flights in 14 days were performed between 25 March and 10 April 2014. In this work, we used only the data measured within the 30-km distance of the SMEAR II Hyytiälä station to enable the comparison with the ground-based data. These include all the flights of the early spring campaign in 2014 and the vast majority of the flights of late spring campaign in 2013. The remaining flights in 2013 were flown near Jämijärvi airport (80 km west from Hyytiälä) together with the Zeppelin NT airship flights during the PEGASOS campaign (Manninen et al, in preparation). Table S1 in the supplementary material presents the descriptive summary of all flights.

During both campaigns, two flights per day were usually performed when weather conditions allowed flying. Due to limitations of Visual Flight Rules (VFR) conditions, the observations were biased towards clear sky and broken cloudy conditions without precipitation and high winds. For flight planning, we used a method by Nieminen et al (2015) to forecast the NPF event probability for Hyytiälä site. In this method, the forecasts for weather, air mass origin, and air quality, as well as the statistics from the long-term data sets were utilized to predict the occurrence of the NPF events during the following days. Although the method could not predict the exact starting time of the NPF, which varied for example with the season and meteorological conditions, the morning flight was planned to coincide with the time when the NPF was expected to start based on long-term observations at the SMEAR II site (Nieminen et al. 2014). The second flight of the same day took place usually 2–3 hours after the first one.

The Cessna airplane was based at Tampere-Pirkkala airport (EFTP), approximately 60 km SW from Hyytiälä. A typical research flight lasted between two and three hours, and it covered an area of several tens of kilometres around Hyytiälä station up to the altitude of 3800 m. The flights were often flown along a line track that was perpendicular to the wind. Along that line, the flight track often consisted of several constant altitude flight legs inside and above the PBL, and a climb up and descent from the top altitude. Most of the research flights were flown in the approximately south-north direction, and the flight routes were chosen to prefer the forested areas and to avoid local sources of anthropogenic emissions. There was a trade-off between the spatial and temporal coverage; when the flight track covered a large area both horizontally and vertically, it could not catch rapid changes at one location.

## 2.4 Ground-based instrumentation

The ground-based measurements were performed at the SMEAR II station in Hyytiälä, Finland (N 67° 45.295', E 29° 36.598', 181 m a.s.l. See Hari and Kulmala, 2005). It is a rural background station in the Finnish countryside, and its surroundings are a mosaic of boreal forests, lakes, agricultural land, wetlands, small roads, small towns or villages and small industrial sites. Fig. 2 presents a land use map near the station. (EEA 1997, Williams et al. 2011). Coniferous or mixed forests cover 66 % of the land area within 50 km from Hyytiälä. The nearest big city, Tampere, is 50 km south-west from Hyytiälä. All altitudes



presented in this paper are meters above the sea level, m a.s.l. The land elevation in the area around Hyytiälä is between 95 and 190 m a.s.l. (data from National Land Survey of Finland, <http://www.maanmittauslaitos.fi/en>)

The description of the continuous ground-based measurements at the SMEAR II Hyytiälä station can be found e.g. from Hari and Kulmala (2005). The Differential Mobility Particle Sizer (DMPS, Aalto et al. 2001) with particle diameter range of 3–800 nm and temporal resolution of 10 minutes was situated inside a research cottage. Its sampled 8 m above the ground level inside the canopy of the boreal forest. Particle concentrations were corrected to STP conditions similarly as the airborne data.

The wind speed and direction were measured at the altitude of 16.8 m above the ground. In addition to meteorological data measured at the Hyytiälä station, we used the Finnish Meteorology Institution's (FMI) measurement network to obtain data on the cloud cover around the area. The cloudiness (with the scale of 1/8–8/8) and the altitudes of the cloud base are measured at Tampere-Pirkkala and Halli airports, which are situated 60 km southwest and 30 km east from Hyytiälä, respectively.

The High Spectral Resolution Lidar (HSRL) was used detect the vertical structure of the troposphere with focus on the aerosol layers, and determine the PBL height above Hyytiälä. The system provides aerosol optical depth, volume backscatter coefficient, cross section, and depolarization profiles with high temporal and vertical resolution (Eloranta 2005). These quantities can be used for example in identifying the dominant aerosol type for different layers using a combination of lidar ratio and depolarization (Li et al. 2009, Petzold et al. 2009).

## 2.5 Data analysis

### 2.5.1 Median vertical aerosol profiles

Statistics of the aerosol vertical profiles were calculated separately for the late spring 2013 and the early spring 2014. Observations of the total number concentrations, and the number concentrations of 10–25 nm and 80–400 nm size bins, which represented the nucleation mode particles and CCN size particles, respectively, within 30 km from Hyytiälä were included. The altitude range of 300–3800 m a.s.l. was divided into 100 m bins, and the medians together with 10<sup>th</sup> and 90<sup>th</sup> percentiles (P10 and P90) are shown in Fig. 3. These vertical profiles were compared to the particle number concentrations and the number size distributions measured simultaneously with the DMPS at Hyytiälä. Additionally, since the flight tracks varied and not all altitudes were covered equally, the relative number of data within each altitude was plotted to show the strength of the statistics.

### 2.5.2 Connecting the airborne and the on-ground measurements: horizontal variation

The ground based aerosol measurements are often generalized on various scales to represent the conditions in a regional scale in the PBL. Using airborne data, we tested this assumption for the Hyytiälä station.

To compare the aerosol size distributions observed on the ground to airborne measurements, log-normal distributions were fitted to the size distribution data from both data sets (Hussein et al. 2005). After fitting, every size distribution was reduced to a sum of 1–3 log-normal distributions. Each of them was defined by three parameters, namely the mode peak diameter, the



mode width, and the concentration of particles in the mode. The error of the fitting was defined to be the difference of the total concentration between the fitted and measured distributions.

The airborne uCPC and SMPS measurements performed inside the PBL were compared with the simultaneous ground-based DMPS measurements. The studied quantities were the total number concentration, as well as the concentrations of 10–25 nm and 80–100 nm particles, as well as particle mode diameters obtained from the mode-fitting algorithm. The uCPC total concentration was averaged to the same 2-min resolution as the SMPS data. This reduces both the random noise and auto-correlation of the data. The 2-min time resolution with the 35 m/s airspeed corresponds to the spatial resolution of 4.2 km. In addition, the Hyytiälä DMPS data were interpolated to the same 2-min grid used with the airborne data. The analysis covered airborne data within 30 km radius from Hyytiälä, and the data were divided into 5-km geographical distance bins.

10 The differences between airborne and on-ground concentrations are presented in Fig. 4a,c,d as a ratio between the airborne number concentration minus ground based, divided by the ground based number concentration. We calculated the median, 10<sup>th</sup> and 90<sup>th</sup> percentiles (P10 and P90, respectively) of these relative difference distributions as a function of the distance where the airborne measurement was performed. For particle diameters (Fig. 4e,f) we compared the absolute differences. We did that for the mode peak diameter of the mode with the largest concentration, and for the smallest mode peak diameter when it was below 25 nm in Hyytiälä.

### 2.5.3 New particle formation event days

Based on the Hyytiälä DMPS data, the days were classified into NPF event days, non-event days, and undefined days (Buenrostro Mazon et al. 2009, Dal Maso et al. 2005, Kulmala et al. 2012). During the NPF days, a new mode of the freshly formed particles (<25 nm) were seen to appear and later grow towards larger particle diameters. During the undefined days, one could see a new mode of small particles but no growth, or a new mode of growing particles was seen but the particles were larger than 25 nm. During the non-event days neither growth nor a freshly-formed small particle mode was seen.

Additionally, the NPF days were divided into classes I and II based on how clear the growth was and if the growth rate and formation rates could be calculated based on the DMPS data (Dal Maso et al. 2005). If the growth of the particles was smooth enough so that the growth rate and formation rate could be estimated, the day was classified into the class I. During these days the NPF was assumed to be homogenous in the regional scale. If there was a clear growing particle mode but the concentration fluctuated so much that these parameters could not be quantified, the day was classified into the class II event.

During the campaign in 2013, in total four class I NPF event, 13 class II NPF event, 11 undefined, and 2 non-event days were observed. The corresponding numbers during the early spring 2014 were 11/2/1/0 (Supplementary material Table S1). One should, however, note that the flights were limited to relatively fair weather days and that biases the data towards the increased NPF probability.



To compare the overall picture and the spatial variation during the class I NPF events, we calculated the differences for each of flights that were flown on the class I NPF days. We show tabulated number concentration ranges for both airborne and on-ground data, and median relative differences over the flights. Furthermore, we collected the airborne data inside the PBL and within a 30 km geographical distance from the SMEAR II station.

#### 5 2.5.4 Selecting case studies

Summary statistical values offer general patterns of phenomena, but detailed information is lost. Therefore, four case studies were selected to show a more precise picture of the vertical and horizontal variation and evolution of selected events.

The case studies illustrate four different NPF situations covering the variability observed during both 2013 and 2014 campaigns. Case I) was 28 March 2014: a class I NPF event day with a rapid nucleation burst and airborne horizontal variation  
10 in concentration. Case II) was 16 May 2013, a class II event day which means inhomogeneous growth and spatial variation in the particle concentration. Case III) on 4 April 2014 was an early hours flight after a NPF day with observed small particles in the residual layer, and case IV) 26 March 2014 was a weak class I NPF day inside the PBL, and with particle growth also in the free troposphere. In addition, we expanded case IV) and showed the frequency and features of all the cases when <25 nm particles were observed in the free troposphere.

### 15 3 Results and discussion

#### 3.1 Median vertical profiles

We compared the vertical profiles of total particle number concentration, and the number concentration in 10–25 nm and 80–400 nm size bins (Fig. 3). The median profiles for these size ranges differed largely from each other between the late spring 2013 and early spring 2014 data. The early spring profile had higher and relatively constant total number concentrations (3000–  
20 4000 cm<sup>-3</sup>) up to the top of the PBL at 1100 m a.s.l. altitude, and above that the concentrations were below 1000 cm<sup>-3</sup> all the way up to 3800 m a.s.l. The same shape can be seen also for the 90<sup>th</sup> percentile (P90) of the concentration profile. During the late spring, the median concentrations at low altitudes were lower than during the early spring, and no similar sharp decrease in the concentration profile can be seen. The aerosol number concentrations decreased continuously all the way up to the altitudes of 3000 m a.s.l. resulting in larger concentrations above 1100 m than during the early spring.

25 We can identify three processes affecting the shapes of the median profiles. Firstly, the measured height of the PBL varied more during the flights in the late spring 2013 (range 350–2560 m a.s.l.) than in the early spring 2014 (range 550–1770 m a.s.l.). This smoothed the median profile of 2013. Secondly, during the early spring 2014, a higher fraction of the measurement days was classified as NPF days, and thus the particle concentration inside the boundary layer was higher compared to the late spring 2013, when the majority of the days were either class II NPF days or undefined days. Thirdly, the high pressure that  
30 prevailed during many of the days in the 2014 campaign caused a large-scale subsidence preventing the mixing between the



PBL and the FT (Hamburger et al. 2011). This blocked the particles rising from the PBL upwards and reduced the concentrations in the FT.

Figure 3c shows the vertical profile of nucleation mode particles in the size bin of 10–25 nm. During the early spring 2014 the nucleation mode number concentration was similarly enhanced as the total concentration when compared to the late spring 2013 profile, which was due to a higher number of class I NPF days. During 2013 polluted air masses dominated resulting in larger concentrations of 80–400 nm particles than during 2014 when air masses were cleaner (Fig. 3d).

When comparing the number concentrations at the lowermost airborne measurements altitudes between 300 and 500 m a.s.l. to those at the ground level, the airborne values were in line with the on-ground values (Fig. 3). For the total number concentration, the airborne median values were 1–88 % larger than the corresponding on-ground values. For 10–25 nm and 80–400 nm particles, the relative differences between the airborne and on-ground concentrations at 300–500 m a.s.l. were in the ranges from –7 % to +121 % and from –17 % to +49 %, respectively.

When looking at the P90 profiles of the concentrations, a high vertical variability can be seen. For example, for 10–25 nm particles during the early spring 2014, the P90 value of the concentration peaked intensively at the altitude of 1100 m ( $10\,500\text{ cm}^{-3}$ ), whereas the concentration at the altitude of 900 m was much lower ( $7800\text{ cm}^{-3}$ ). This was at least partly explained by the contributions that the different flights had to the each altitude-bin's data. The altitude-bins of 300 m and 1100 m were dominated by intense NPF days, whereas the data for altitude-bins of 400 m and 900 m included both intense and weaker NPF days.

### 3.2 Representativeness of on-ground data

We compared the flight measurements inside the PBL and ground-based observations in Hyytiälä with a focus to find out how well the measurements in Hyytiälä represent the particle concentration and size distribution horizontally. As seen in Fig. 4a, the differences between airborne and ground-based measurements were relatively small for the total aerosol number concentration. When comparing the medians, the airborne total number concentrations were 0–17 % larger than the ground-based concentrations during the 2013 campaign (blue lines), whereas the airborne concentrations were 13–26% larger during the 2014 campaign (red lines). The variability (P10 and P90) was between –68 % and +114 %. The flat median curves indicate that, on average, the particle number concentration was relatively constant over the area of 30 km. However, the variability grew as a function of the distance, as shown by the rising P90 curves.

The median relative differences in the concentration of the nucleation mode particles (10–25 nm) showed that their concentrations were 6–82 % higher airborne than on the ground Fig. (4c). Smaller particles have shorter lifetimes and have sources closer to the measurement point than larger particles, which explains the higher variability of the concentration of 10–25 nm particles than that of larger particles. For the sub-25 nm particles, the relative difference was larger during the early spring 2014 that had a high fraction of NPF days compared with 2013. The P10 of the difference between the ground level and



airborne concentrations of 10–25 nm particles was between –80 % and +5%, whereas the P90 curves show that the airborne observations could be up to 108–350 % larger than on-ground. The range of relative difference (P90) increased as a function of distance from Hyytiälä, which indicated that the range of variability was still evolving as the distance grows.

The horizontal profiles of the larger accumulation mode particles in the size range of 80–400 nm showed very low (from –2 % to +6 %) median differences between the airborne and on ground values for both early and late springs (Fig. 4d). This feature is connected to the longer lifetime of these particles.

In addition to concentrations, we compared the mode peak diameters of the modes with the largest concentration (Fig. 4e), and the smallest modes when there was a <25 nm mode in Hyytiälä (Fig. 4f). For both cases, the mode peak diameters of both nucleation mode and the largest mode agreed very well over all distances from Hyytiälä. When looking at the most dominant mode, the airborne particles were slightly, from –2 nm to –10 nm (median values), smaller than the particles measured in Hyytiälä. The median difference for the nucleation mode diameter was from –1.7 nm to +0.3 nm and P10–P90 variation between –12 nm and 26 nm. For both modes, the late spring 2013 was found to have a larger variability than the early spring 2014, which was consistent with the higher number of class II and undefined days in the late spring.

In general, the total number concentration and the concentrations of 10–25 nm and 80–400 nm particles were higher airborne than on-ground. The measurements in Hyytiälä were performed within the forest, so these differences were likely partly due to the dry deposition of particles onto the forest canopy. The mode peak diameter comparison indicated smaller particles airborne than on ground level. This is hard to explain by aerosol processes and might be due to a slight instrumental discrepancy between the airborne SMPS and Hyytiälä DMPS.

### 3.2.1 Class I NPF days seen on the ground and from the aircraft

To explain the regular growth the particles during the class I NPF events, a homogenous air mass is often assumed to cover a large area. We tested this by comparing the median differences between the ground level and airborne measurements calculated over the campaigns in the previous section, to the median differences during the class I NPF days. The late spring 2013 flights were performed on three class I event days, and the early spring 2014 flights on eight days.

The median differences of the airborne and ground based concentration values for each flight are presented in Table 3. The absolute P10 and P90 ranges (rounded to the closest hundred particles) are shown in supplementary material in Table S2. For class I event days in 2013 the airborne total number concentrations were 17–34 % larger than the concentrations on the ground (median values), whereas for all data in 2013 the median difference was smaller (9 %, Fig. 3b). In 2014, the median values of the total number concentration difference during class I NPF days varied between –1 % and +99 % (average was 40%) in favour of airborne observations. The median difference over the 2014 campaign was smaller, 11%. The differences of the 10–25 nm particle concentrations on the class I NPF days were quite similar to that in all days. In the majority of the days, the median differences between airborne and on-ground measurements of both the total number concentration and 10–25 nm



particle concentrations were larger during the morning flight when NPF had just started, than during the afternoon when the PBL mixing had had more time to smooth out the differences.

When comparing the mode peak diameters of the nucleation modes during the class I NPF days, the median diameters of the airborne particles were typically 2–3 nm smaller than on-ground. This is a quite similar value than the medians over all data during the campaigns.

### 3.3 Case studies

New particle formation is a complex phenomenon, and not fully understood. Variability in aerosol number concentration in time and space is high, especially during the early stage of NPF. Therefore, in this section several case studies are analysed to show how a NPF event is seen from both airborne and ground based perspectives simultaneously. Key parameters related to the NPF observed at the ground level for these cases are collected to Table 2.

#### 3.3.1 28 March 2014: Rapid and intense NPF

A strong NPF day with intensive formation and rapid growth of particles was observed on clear-sky day, 28 March 2014. Although the sky was clear, there was a humid layer with elevated water vapour concentration at the altitude of 2700–3200 m a.s.l. (Fig. 5e, mixing ratio of water vapour, H<sub>2</sub>O MR, 3.1–4.2 mmol/mol inside the layer vs. <1 mmol/mol below it). The average wind speed in Hyytiälä was 1 m s<sup>-1</sup> and the wind direction was changed from easterly wind in the morning to north-west in the afternoon. The air mass originated from North and from above the Arctic Ocean. The meteorological conditions of the day made a good prerequisite for NPF event. During the morning flight, the PBL height was observed to rise from 700 m to 1180 m a.s.l., and during the afternoon flight it was around 1060 m a.s.l.

At the ground level, the beginning of the NPF was observed at 10:50 with a strong burst when particles with a wide range of diameters (4–25 nm) appeared (Fig. 5a). The formation rate of 3 nm particles, J<sub>3</sub>, during the event was 3.9 cm<sup>-3</sup>s<sup>-1</sup> and the growth rate (GR<sub>3-25 nm</sub>) was 4.0 nm/h until around 13:00. After that, the mode peak diameter remained rather stationary (30 nm) until 16:30.

The first flight of the day was conducted in the vicinity of Hyytiälä between 10:05 and 12:15, and thus the measurements were performed just before and after the NPF started on the ground. Figs. 5b–f show the quantities measured on-board of the Cessna. The flight profile consisted of an ascent up to the flight level 120 (~3.8 km) and a descent, together with one constant altitude flight leg during the rise and four flight legs during the descent, all headed with the NNW–SSE direction (Figs. 5b–c).

Before the ascent, NPF was not observed inside the PBL, the total concentration was 1000–6000 cm<sup>-3</sup> and the main mode peak diameter was 60–80 nm (Fig. 5c). At 10:20, over the area near Ruovesi (see the map on Fig. 5b), just above the top of the rising convective PBL and below a capping temperature inversion between altitudes of 700 and 1100 m a.s.l., the concentrations reached 12 000 cm<sup>-3</sup> with the mode peak diameter of 28 nm. This was over half an hour before the NPF was observed at Hyytiälä. Due to the distance of 15–20 km from Hyytiälä, the direct connection between this event and NPF that occurred in



Hyytiälä later is not obvious, and the data are not sufficient to confirm if these particles indicate the vertical starting point of the NPF. The particles observed just above the PBL were not freshly nucleated, but based on the size of the observed particles, they had likely been formed already several hours before the observations. The previous day had been a NPF class II event day, and then the nucleation mode had grown up to 20 nm before the sunset. The particles above PBL could therefore also originate from previous day's nucleation and, due to the lack of available condensable vapours, had stopped growing in the nocturnal residual layer. Additionally, the first particle size distributions of the nucleation burst observed in Hyytiälä had a bimodal structure with mode peak diameters of 12–20 nm for the second mode, similar to the Aitken mode observed from the aircraft. It is likely that the Aitken mode particles were mixed downward in the growing PBL.

Above the inversion at altitudes of 1100–1700 m a.s.l., the atmosphere was stratified. Particle number concentrations in these layers varied between 3000 and 700 cm<sup>-3</sup>, and sub-15 nm particles were measured with a SMPS (Fig.6). However, the inversion was observed throughout the day at around 1100 m a.s.l., and the potential temperature profiles showed no mixing inside these layers, so there was no indication at the downward transport.

The NPF was fully on-going when the aircraft arrived again at the PBL at 11:33 (Fig. 5c). The airborne total number concentration measured with the uCPC was very high, between 10 000 and 40 000 cm<sup>-3</sup>, and had a notably large variation over short timescales. The mode peak diameter of the particles was below 10 nm. The concentration variation was likely dominated by the smallest particles, although the time resolutions of the SMPS prevented us to study the variation of the size distribution with the same accuracy as with the uCPC.

To better visualize the horizontal and vertical concentration variation, we projected the flight track along the NNW–SSE direction line, and plotted the total particle concentration and water vapour mixing ratio along this line and as a function of altitude (Figs. 5d,f). There were areas of enhanced aerosol number concentrations more than 4 km wide and 12 km from each other. The total number concentration was over four times higher in these areas than in surroundings. Higher aerosol number concentration were associated with higher values of the water vapour mixing ratio (Figs. 5d,f). The source of water vapour is at the surface from evaporation and evapotranspiration. With mixing and convection in PBL the air is lifted to upper parts of boundary layer together with gaseous precursors needed for new particle formation. Areas with intensified updraft convection might thus be linked to the areas of intensified NPF. The decreasing temperature and pressure during the uplifting of the air will contribute to enhanced nucleation. Direct airborne observations of vertical wind and trace gases were not available and this hypothesis needs further experimental targeted study.

The second flight of the day took place around Hyytiälä between 14:35 and 16:20 (Figs. 7). During the flight, the particle number size distribution in Hyytiälä remained relatively stable with a number concentration of 13 000 cm<sup>-3</sup> and mode diameter of 26 nm. According to the airborne measurements, the number concentration inside the PBL varied between 13000 and 23000 cm<sup>-3</sup>, and the mode peak diameters were between 22 and 29 nm. Similar to the morning, the areas with high particle concentrations throughout the PBL occurred also in the afternoon. The average concentration in these areas was, however,



only 1.5-fold compared to the areas around them, while it had been 4-fold in the morning. This was likely due to the PBL mixing, which had diluted the concentration differences of vapours and particles.

### 3.3.2 16 May 2013: Irregular NPF day

The second case study day represents a class II event day. Such days, together with undefined days, were the most common cases during the spring 2013 campaign. The difference between class I and II NPF event days is that on class II days the growth of the nucleation mode particles observed at the ground level is irregular so that neither the formation nor growth rate can be calculated. Therefore, the air mass is not as homogeneous on class II event days as on the class I NPF days. We concentrate on one example case of class II events, 16 May 2013, to study the spatial inhomogeneity.

On 16 May 2013, prevailed clear-sky conditions. The ground temperature during the morning flight was in the between 17–18 °C and during the afternoon it was about 20 °C. The wind was from southeast and the average wind speed was 2 m/s. The studied air mass was advected from southeast. The high air temperature resulted in a high PBL: the top of the PBL increased from 540 m a.s.l. at 08:12 up to 1920 m a.s.l. before 14:15.

A 30-minute burst of sub-10 nm particles was detected starting at 9:07 on the ground (Fig. 8a). The morning flight was near Hyytiälä between 08:30–10:40. The first observations of this burst were made at 09:01 inside the PBL at the altitudes of 1145–670 m a.s.l. Although the first panel of Fig. 8c show that high concentrations were observed just below the top of the PBL, the remaining flight path (Fig. 9a) reveals that the burst was horizontally, not vertically limited to the upper parts of the PBL. High concentrations were measured at all altitudes through the PBL, and the burst had a width of 20 km (Fig. 8e). The total particle number concentration measured at the ground during the burst was 2800 cm<sup>-3</sup>, which was around half of the airborne peak values. The particles inside the PBL were mainly smaller than 10 nm, but due to the limitations of the SMPS size range, it is not possible to give the variation of the nucleation mode diameter. During the flight, a spiral descent near Hyytiälä was performed (Fig. 8c, starting at 10:05, the spiral starting at 2000 m a.s.l. in Fig. 9a). This descent offers a vertical profile with a temporal resolution of 15 min. Slightly larger concentrations (4000 cm<sup>-3</sup>) were obtained at altitudes of 1200–1700 m a.s.l. than below them (3500 cm<sup>-3</sup>).

The afternoon flight (14:15–16:05) was flown simultaneously with the day's highest particle concentrations measured in Hyytiälä. According to the airborne measurements in the PBL, the surroundings of Hyytiälä were clearly divided to two different areas (Fig. 8f and Figs. 9b,d) and the Hyytiälä measurements did not represent the area around it. The particle number concentration at the ground level in Hyytiälä was between 4300 and 5500 cm<sup>-3</sup> and airborne above it 5000–6000 cm<sup>-3</sup>. Over the areas south from Hyytiälä the concentration was around 2000–4000 cm<sup>-3</sup>, whereas in the northern part of the area the concentration was peaking with values up to 6000–10000 cm<sup>-3</sup>. The particles in the northern part of the area had slightly larger mode peak diameter (16–20 nm) than the particles in the southern part of the area (below 10 nm – 17 nm). The northern area with the higher concentration was also slightly less moist (H<sub>2</sub>O MR 4.4–4.6 mmol/mol) compared to the southern area



(4.8–5.3 mmol/mol) (Fig. 9d). Additionally, inside the northern area the most elevated concentrations were found at altitudes above 1000 m a.s.l.

This case day shows that the temporal variation observed on the ground was only partly connected to the spatial scales of the advected air mass. When looking the Hyytiälä DMPS data, the first burst and the subsequent lack of the nucleation mode particles had very different durations: 0.5 and 3.5 hours. With a wind speed of 2 m/s these time scales would correspond to the spatial scales of around 1 km and 10 km, respectively.

### 3.3.3 4 April 2014: A nocturnal flight after a NPF event day

During the March–April 2014 campaign, one flight was performed to observe aerosols in the nocturnal boundary layer (Fig. 10). The flight took place on 4 April 2014 between 03:40 and 05:10 in the surroundings of Hyytiälä. The sunrise occurred after the flight, at 05:39. During the flight, no clouds were observed at the Halli airport, whereas at the Tampere-Pirkkala airport the cloud cover was reducing from 7/8 to 1/8 and the cloud base was observed to descend from 2600 m to 2000 m. The HSRL lidar in Hyytiälä showed drizzle that evaporated at the altitudes of 700–1900 m a.s.l. (Fig. 10d), and no precipitation was measured at Hyytiälä. The wind speed was below 1 m/s.

In Hyytiälä a growing mode of particles, originating from previous day's nucleation, was clearly observable (Fig. 10a). The mean peak diameter of this mode was between 25 and 27 nm and the particle number concentration varied between 3100 and 3800 cm<sup>-3</sup>. Because of the structure of a nocturnal PBL, the lowermost surface layer was assumed to be very thin, approx. 100 m (Garratt 1992), and not connected to the above layers.

During the flight, three areas with different aerosol characteristics could be observed (see map Fig. 10b). North from Hyytiälä the particle number concentration exceeded 4000 cm<sup>-3</sup> and the mode peak diameter of the smallest mode was between below 10 nm and 30 nm. There is a sawmill nearby in the Vilppula village, and the observed enhanced aerosol load was possibly related to sawmill emissions.

North-east from Hyytiälä, there was an area with particle number concentrations between 3000 and 4000 cm<sup>-3</sup>, and with the smallest mode peak diameters varying from slightly below 10 nm up to 20 nm. These measurements were vertically limited between the altitudes of 800 and 2000 m a.s.l. and connected to a slightly more humid layer (H<sub>2</sub>O MR 2.0–2.6 mol/mol) than the area near Vilppula or south-west from Hyytiälä. As seen from the lowest panel of Fig. 10c, the particle number concentration and H<sub>2</sub>O MR followed each other. We speculate that these small particles originate from the previous day's NPF event. The height of the PBL had been 1800 m a.s.l. during the previous day's afternoon flight at around 14:00, and thus the altitudes of 800–2000 m a.s.l. were inside the nocturnal residual layer (Stull 2012). The sunset on 3 April 2014 had been at 19:16, which is marked to the Hyytiälä DMPS plot as a dotted line. At that time, the mode peak diameter in DMPS had been 13 nm and the number concentration 3400 cm<sup>-3</sup>. After the sunset, the mixing ended, and no more vapours were transported up from the surface. This had probably stopped the growth of the particles in the nocturnal boundary layer. The sizes and the concentrations of the observed particles fit this hypothesis.



South-west from Hyttiälä the particle number concentration was between 1000 and 3000 cm<sup>-3</sup> and the mode peak diameter was small, below 10 nm. The H<sub>2</sub>O MR was rather stable between 1.3 and 1.8 mmol/mol. The measurement are from the 440–500 m a.s.l. altitudes. The flight path was under a cloud and the larger submicron particles could have been scavenged by the drizzle from it.

### 5 3.3.4 26 March 2014: Weak NPF in the PBL and FT nucleation

The third case study was a weak class I NPF day, 26 March 2014 (Fig. 11a). Two flights took place, the first one flying in the vicinity of Hyttiälä between 10:25 and 12:25 and the second one between 15:10 and 17:10. The sky was clear during all the day. The ground temperature during the morning flight was 6–8 °C, and it decreased during the afternoon flight from 10 to 4°C. The average wind speed during both flights was 2 m/s from NE. The PBL height was around 650 m a.s.l. on the first ascent, and rose before the second flight to 900 m a.s.l. (Fig. 11b).

During the morning flight (Figs. 12a,c,e) a 25 km-long horizontal flight leg at the altitude of 400 m a.s.l. was first performed. This was followed by an ascend to 3.7 km and a descent. During the first leg, at 10:39, a small area of particles with diameters smaller than 10 nm was observed 2 km south from Hyttiälä. The total particle number concentration in this area was between 2000 and 6000 cm<sup>-3</sup> and outside of it around 1400 cm<sup>-3</sup>. The airborne concentrations of uCPC and integral SMPS followed each other, which indicates only a small number of 3–10 nm particles. The first signs of NPF were observed in Hyttiälä at 10:40 but the total particle concentration was only 900–1400 cm<sup>-3</sup>, and the nucleation mode remained very weak until 12:30. After entering back in the PBL at 12:05, a clear mode of particles with diameter less than 10 nm was seen with the SMPS, and the difference between uCPC and SMPS was observed as a sign of on-going NPF. The total concentration varied with a factor of four from 1500 to 6000 cm<sup>-3</sup>. In Hyttiälä, freshly formed particles with a mode peak diameter of 6–8 nm were detected, which is in line with the airborne measurements.

Additionally, there was an area of elevated particle concentrations 15 km north from Hyttiälä just below the boundary layer top (Fig. 12e). The same spot was observed twice, both when ascending and descending with the 1.5-hour time difference. Although the flight track did not allow us to get information on that location at lower altitudes, 1.5 hours is more than the typical mixing time of the PBL due the convection, and thus the spot was more probably a spatial hot spot than an altitude with higher concentrations.

During the second flight, the nucleation mode particles inside the PBL were seen to grow from average 11 nm to 14 nm within an hour, and thus their average growth rate was 3 nm/h (Fig. 12b). The average growth rate observed in Hyttiälä during that day's event was 2 nm/h. The airborne concentrations in the PBL during the afternoon flight varied between 4000 and 10000 cm<sup>-3</sup>.

In addition to the nucleation in the PBL, a layer of sub-25 nm particles was measured during the morning flight on 26 March 2014 between the altitudes 2000–2800 m a.s.l. (Figs. 12a,e). The calculated potential temperature (Fig. 11b) showed that these altitudes were above the mixing PBL and the residual layer, and thus inside the free troposphere (FT). The layer was clearly



observed by the uCPC (cut-off 3 nm), but hardly at all detectable by the SMPS (size range 10–400 nm), which indicates that the particles had diameters smaller than 10 nm. The total particle number concentration inside the layer was 2000–6000 cm<sup>-3</sup>, whereas outside of it the concentration was 200–1000 cm<sup>-3</sup>.

The FT layer was still observable during the afternoon flight, now between the altitudes of 1800–2400 m a.s.l. with the particle concentration of 3000 cm<sup>-3</sup> (Figs. 12b,d). The particles in the layer grew, and the mode was clearly visible in the SMPS data, although the mode peak diameter was still below 10 nm. Assuming that the diameter of the particles was at least 3 nm in the morning, and no larger than 10 nm in the afternoon, and that the time difference between the observations was around four hours, we can calculate that the growth rate of the particles was well below 2 nm/h.

The HYSPLIT back trajectory calculations performed for the time of the earliest observation of the small FT particles (11:00 Local time=09 UTC), showed that the air above the PBL originated from north, had descended from higher parts of the free troposphere during the previous 1.5 days, and had been connected with ground for 2.5 days before arriving to Hyytiälä (Fig. 13a). In the previous day (25 March 2014) at 12:00 UTC, the air mass had been approximately over the Norwegian coast and above 5000 m a.s.l. A simultaneous satellite image on 25 March 2014 at 11:55 UTC (Fig. 13b) shows that a cloud edge was reaching that area. Thus, the air masses entering at Hyytiälä on 26 March 2014 at 11:00 LT and later that day had most likely passed through cloudy region a day before. Additionally, the sounding profile measured from Hyytiälä at 13:24 (Fig. 13c) shows a local horizontal wind speed maximum between altitudes 2100–2700 m a.s.l, which indicates enhanced turbulence. SMPS data showed reduced condensation sink values inside the NPF layer (Fig. 13a). We assume that first the air had been lifted up to the free troposphere together with precursor gases from ground or ocean, so that wet scavenging inside the cloud had decreased the condensation sink of the air mass, which together with turbulent mixing would have favoured nucleation. The time the air mass had spent above the PBL, 2.5 days, has been long enough for the vapours to oxidize and comparable those reported by Bianchi et al (2016).

### 3.4 Free troposphere NPF

During both of the campaigns we observed layers of newly formed particles in the free troposphere similar to the event observed on 26 May 2014 (see Table 4). During the late spring 2013 campaign, we observed these layers on nine days of the total 26 flight days with measurements at the altitudes of 2 km or higher. Six of these cases were morning flights, and we did not observe the same layers with enhanced aerosol concentrations during the afternoon when there was a second flight. The mode peak diameter of these particles was typically in the range of 15–20 nm. When comparing the backward air mass trajectories and satellite images, we observed that for eight daytime cases the air mass had passed a cloudy region associated with frontal systems between 12 and 20 hours prior to observations. Also, based on the trajectory analysis, the studied air masses were advected from the PBL into the FT within 16–70 hours before arriving to Hyytiälä. In one third of the cases, the 96-hour backward trajectories did not show lifting from the PBL. In four out of nine cases the condensational sink from SMPS



data were reduced in the layer with enhanced number density of small ultrafine particles. This is likely an indication of aerosol scavenging in the clouds.

During the early spring campaign 2014, similar layers with enhanced ultrafine aerosol number density were detected on seven days out of the total 10 days with sufficient data. Typically, these layers were observed during both the morning flight (five cases) and again during the afternoon flight (four of these five cases). During the morning flight the ultrafine mode had the diameters up to 15 nm. Before the afternoon flight the mode diameters had grown 5–15 nm and the mode had reached the sizes of 10–25 nm. Of these seven days, the air masses had passed cloudy areas in five cases within 12–24 hours, and the air mass was lifted from the PBL to the FT 18–60 days before arriving at Hyytiälä. In two cases the air mass most likely had not been in contact with the PBL during the last 96 hours. In 4/7 cases the a removal of accumulation mode particles and decreased condensational in the layer was observed.

The observations from all NPF cases in the free troposphere strengthen the hypothesis formed from case study. An air mass had had vapours originating from ground or ocean up into the free troposphere 0.5-3 days before the air mass had been observed. According to Bianchi et al (2016), in Central Europe 1-2 days is required for the oxygenation processes to produce enough condensable molecules. Possibly lower vapour concentrations or sun radiation in Northern Europe might lengthen this time. In the free troposphere, the air mass had passed through a cloudy area, which had decreased its condensational sink and promoted NPF.

#### 4 Summary and conclusions

The main focus of this work was to investigate 1) the spatial and temporal variability of aerosol number density and size distribution in the planetary boundary layer and the lowermost free troposphere and 2) the variability and magnitude of new particle formation in the PBL, and 3) to asses the representativeness of the ground based observations at Hyytiälä for PBL aerosol distribution of spatial scale of tens of kilometres. This work is based on an extensive data set of 111 flight hours.

The spring 2013 campaign was dominated by polluted air masses with high background aerosol loadings, while the following spring campaign in 2014 was carried out during clean conditions of marine and Arctic air masses. Although the total aerosol number concentration in both campaigns were around 2000–3000 cm<sup>-3</sup> in the PBL, during the 2013 campaign the concentration of particles with diameters in the range of 10-25 nm was only 20-50 % of those in the range of 80-400 nm. In the 2014 campaign, in contrast, the concentration of the 10-25 nm particles was four to seven times higher than the concentration of the accumulation mode particles.

On a statistical basis, the aerosol number density in the air masses within 30 km from Hyytiälä differed only slightly from the ground-based observations in Hyytiälä. The PBL average total concentrations were about 10 % higher than the concentrations at the ground level. The canopy losses can explain this partly, since the measurements at ground were performed inside a



coniferous forest. The concentration of nucleation mode particles was around 40 % (median relative difference) higher aloft than on the ground, and the variability of the differences was larger than for the accumulation mode particles.

Airborne campaigns were limited to the spring period, and the measurement flights were conducted only during fair weather days. Results presented here should therefore be considered as ‘snapshots’ of the real variation inside the campaigns, and  
5 generalization outside of these campaign periods should be done with care.

Even when the NPF was observed to be relatively homogeneous at the ground, there was notable variability in the newly formed particle concentrations on a scale of couple tens of kilometres in horizontal scale. The case day 16 May 2013 demonstrated that the inhomogeneity in the NPF and growth of the particles during the class II NPF event day observed at a fixed station can be linked to spatial differences in the air mass. The horizontal fluctuations were found to be larger than the  
10 differences in the vertical profile. However, the total number concentration was found to be 15% larger at the upper part than in the lower part of the of the PBL, although it was measured 1.5 hours after the first signs of the NPF were observed at ground, and thus the boundary column was expected to be mixed. The flights not presented in details here were in line with the case studies. Horizontally separated NPF ‘hot spots’ were a common phenomenon. The spatial extent of these hot spots along the flight paths varied from a couple of kilometres to more than 20 km.

15 The measurements showed neither a clear enhancement of small particles at the entrainment or residual layer before the nucleation started nor could exclude it. This was due to the low vertical resolution of the flight patterns, and the difficulty into predicting the exact starting time of the NPF. The observed horizontal variation in the nucleation mode particles addresses the caution that is needed when interpreting the vertical profiles. If a straight flight path is ascending or descending, a horizontal variation can be mixed with the vertical variation. These results demonstrate the importance of careful flight  
20 planning to collect data at all interesting altitudes.

In the nocturnal and morning atmosphere before the convective mixing, the residual layer was found to be not connected to the surface layer. The residual layer particles did not grow over the sizes they had before the residual layer was formed, meanwhile in the surface layer the particles remained to grow. The reason is likely that the vegetation continued to emit vapours into the surface layer but they could not enter the residual layer.

25 In addition to the NPF in the PBL, nucleation mode particles were measured frequently in the FT. They were observed in all times of the day, but the smallest, i.e. the most recently nucleated particles were detected in the mornings. The total concentration values in the layers with <25 nm particles in FT were between 200 and 5000 cm<sup>-3</sup>. Based on the air mass trajectory and satellite data of clouds, the majority of the nucleating air masses in the FT had lifted up into the free troposphere 0.5-3 days before, and then had passed a cloudy area 12–24 hours before arriving to Hyytiälä.

30



## Data availability

The measured airborne data is available upon request. Hyytiälä SMEAR II data is available through AVAA open research data portal (<http://avaa.tdata.fi/web/avaa/>). The satellite images were directly retrieved from the website of Dundee University (<http://www.sat.dundee.ac.uk/>) and air mass trajectory data were from NOAA (<http://ready.arl.noaa.gov/HYSPLIT.php>).

5 Atmospheric sounding data and HSRL Lidar data are available from ARM Data Archive [arm.gov](http://arm.gov).

*Acknowledgements.* This work was supported by the Office of Science (BER), U.S. Department of Energy. This research has been funded by the ERC-Advanced "ATMNUCLE" (grant no. 227463), the Academy of Finland (Center of Excellence project no. 272041), the Eurostars Programme under contract no. E!6911 and the European Commission under the Framework Programme 7 (FP7-ENV-2010-265148), and the European Union's FP7 capacities programme under ACTRIS (grant no. 262254), and Horizon 2020 research and innovation programme under ACTRIS-2 (grant no. 654109). In addition, this work was supported by CRAICC and the Swedish Research Councils. The authors would like to thank Airspark Oy and Erkki Järvinen with his crew for flight operation and Pirkko Karlsson from FMI for meteorological data. The authors acknowledge the NOAA Air Resources Laboratory (ARL) for the provision of the HYSPLIT transport and dispersion model and/or READY website (<http://www.ready.noaa.gov>) used in this publication.

## References

- Aalto, P., Hämeri, K., Becker, E., Weber, R., Salm, J., Mäkelä, J., Hoell, C., O'Dowd, C., Hansson, H., Väkevä, M., Koponen, I., Buzorius, G. and Kulmala, M.: Physical characterization of aerosol particles during nucleation events, *Tellus B*, 53, 2001.
- 20 Andrews, E., Sheridan, P. and Ogren, J.: Seasonal differences in the vertical profiles of aerosol optical properties over rural Oklahoma, *Atmospheric Chemistry and Physics*, 11, 10661-10676, 2011.
- Bianchi, F., Trostl, J., Junninen, H., Frege, C., Henne, S., Hoyle, C. R., Molteni, U., Herrmann, E., Adamov, A., Bukowiecki, N., Chen, X., Duplissy, J., Gysel, M., Hutterli, M., Kangasluoma, J., Kontkanen, J., Kuerten, A., Manninen, H. E., Muench, S., Perakyla, O., Petaja, T., Rondo, L., Williamson, C., Weingartner, E., Curtius, J., Worsnop, D. R., Kulmala, M., Dommen, J. and Baltensperger, U.: New particle formation in the free troposphere: A question of chemistry and timing, *Science*, 352, 1109-1112, 10.1126/science.aad5456, 2016.
- 25 Buenrostro Mazon, S., Riipinen, I., Schultz, D., Valtanen, M., Maso, M. D., Sogacheva, L., Junninen, H., Nieminen, T., Kerminen, V. and Kulmala, M.: Classifying previously undefined days from eleven years of aerosol-particle-size distribution data from the SMEAR II station, Hyytiälä, Finland, *Atmospheric Chemistry and Physics*, 9, 667-676, 2009.
- 30 Collins, D. R., Flagan, R. C. and Seinfeld, J. H.: Improved inversion of scanning DMA data, *Aerosol. Sci. Technol.*, 36, 1-9, 2002.
- Crumeyrolle, S., Manninen, H., Sellegri, K., Roberts, G., Gomes, L., Kulmala, M., Weigel, R., Laj, P. and Schwarzenboeck, A.: New particle formation events measured on board the ATR-42 aircraft during the EUCAARI campaign, *Atmospheric Chemistry and Physics*, 10, 6721-6735, 2010.



- Dal Maso, M., Hyvärinen, A., Komppula, M., Tunved, P., Kerminen, V., Lihavainen, H., Viisanen, Y., Hansson, H. C. and Kulmala, M.: Annual and interannual variation in boreal forest aerosol particle number and volume concentration and their connection to particle formation, *Tellus B*, 60, 495-508, 10.1111/j.1600-0889.2008.00366.x, 2008.
- 5 Dal Maso, M., Kulmala, M., Riipinen, I., Wagner, R., Hussein, T., Aalto, P. P. and Lehtinen, K. E. J.: Formation and growth of fresh atmospheric aerosols: eight years of aerosol size distribution data from SMEAR II, Hyytiälä, Finland, *Boreal Env. Res.*, 10, 323-336, 2005.
- Easter, R. C. and Peters, L. K.: Binary homogeneous nucleation: Temperature and relative humidity fluctuations, nonlinearity, and aspects of new particle production in the atmosphere, *J. Appl. Meteorol.*, 33, 775-784, 1994.
- 10 EEA: Technical and Methodological Guide for Updating CORINE Land Cover Data Base, EUR 17288 EN, 1997.
- Eloranta, E. W.: High Spectral Resolution Lidar, in *LIDAR: range-resolved optical remote sensing of the atmosphere*, in: *Lidar: Range-Resolved Optical Remote Sensing of the Atmosphere*, Weitkamp, C. (Ed.), Springer-Verlag New York, 2005.
- Garratt, J.: *The atmospheric boundary layer*, Cambridge atmospheric and space science series, Cambridge University Press, Cambridge, 416, 444, 1992.
- 15 Hamburger, T., McMeeking, G., Minikin, A., Birmili, W., Dall'Osto, M., O'Dowd, C., Flentje, H., Henzing, B., Junninen, H., Kristensson, A., de Leeuw, G., Stohl, A., Burkhardt, J. F., Coe, H., Krejci, R. and Petzold, A.: Overview of the synoptic and pollution situation over Europe during the EUCAARI-LONGREX field campaign, *Atmos. Chem. Phys.*, 11, 1065-1082, 10.5194/acp-11-1065-2011, 2011.
- Hari, P. and Kulmala, M.: Station for Measuring Ecosystem-Atmosphere relations (SMEAR II), *Boreal Env. Res.*, 10, 315-20 322, 2005.
- Hussein, T., Dal Maso, M., Petäjä, T., Koponen, I. K., Paatero, P., Aalto, P. P., Hämeri, K. and Kulmala, M.: Evaluation of an automatic algorithm for fitting the particle number size distribution, *Boreal Env. Res.*, 10, 337-355, 2005.
- 25 Kerminen, V. -, Petaja, T., Manninen, H. E., Paasonen, P., Nieminen, T., Sipila, M., Junninen, H., Ehn, M., Gagne, S., Laakso, L., Riipinen, I., Vehkamäki, H., Kurten, T., Ortega, I. K., Dal Maso, M., Brus, D., Hyvarinen, A., Lihavainen, H., Leppä, J., Lehtinen, K. E. J., Mirme, A., Mirme, S., Horrak, U., Berndt, T., Stratmann, F., Birmili, W., Wiedensohler, A., Metzger, A., Dommen, J., Baltensperger, U., Kiendler-Scharr, A., Mentel, T. F., Wildt, J., Winkler, P. M., Wagner, P. E., Petzold, A., Minikin, A., Plass-Duelmer, C., Poeschl, U., Laaksonen, A. and Kulmala, M.: Atmospheric nucleation: highlights of the EUCAARI project and future directions, *Atmos. Chem. Phys.*, 10, 10829-10848, 10.5194/acp-10-10829-2010, 2010.
- 30 Kerminen, V., Paramonov, M., Anttila, T., Riipinen, I., Fountoukis, C., Korhonen, H., Asmi, E., Laakso, L., Lihavainen, H., Swietlicki, E., Svenningsson, B., Asmi, A., Pandis, S. N., Kulmala, M. and Petaja, T.: Cloud condensation nuclei production associated with atmospheric nucleation: a synthesis based on existing literature and new results, *Atmos. Chem. Phys.*, 12, 12037-12059, 10.5194/acp-12-12037-2012, 2012.
- 35 Komppula, M., Lihavainen, H., Hatakka, J., Paatero, J., Aalto, P., Kulmala, M. and Viisanen, Y.: Observations of new particle formation and size distributions at two different heights and surroundings in subarctic area in northern Finland, *J. Geophys. Res.*, 108, doi:10.1029/2002JD002939, 2003.



- Kulmala, M. and Kerminen, V. M.: On the formation and growth of atmospheric nanoparticles, *Atmos. Res.*, **90**, 132-150, 2008.
- Kulmala, M., Asmi, A., Lappalainen, H. K., Baltensperger, U., Brenguier, J. -, Facchini, M. C., Hansson, H. -, Hov, O., O'Dowd, C. D., Poeschl, U., Wiedensohler, A., Boers, R., Boucher, O., de Leeuw, G., van der Gon, H. A. C. D., Feichter, J., Krejci, R., Laj, P., Lihavainen, H., Lohmann, U., McFiggans, G., Mentel, T., Pilinis, C., Riipinen, I., Schulz, M., Stohl, A., Swietlicki, E., Vignati, E., Alves, C., Amann, M., Ammann, M., Arabas, S., Artaxo, P., Baars, H., Beddows, D. C. S., Bergstrom, R., Beukes, J. P., Bilde, M., Burkhardt, J. F., Canonaco, F., Clegg, S. L., Coe, H., Crumeyrolle, S., D'Anna, B., Decesari, S., Gilardoni, S., Fischer, M., Fjaeraa, A. M., Fountoukis, C., George, C., Gomes, L., Halloran, P., Hamburger, T., Harrison, R. M., Herrmann, H., Hoffmann, T., Hoose, C., Hu, M., Hyvarinen, A., Horrak, U., Iinuma, Y., Iversen, T., Josipovic, M., Kanakidou, M., Kiendler-Scharr, A., Kirkevag, A., Kiss, G., Klimont, Z., Kolmonen, P., Komppula, M., Kristjansson, J. -, Laakso, L., Laaksonen, A., Labonnote, L., Lanz, V. A., Lehtinen, K. E. J., Rizzo, L. V., Makkonen, R., Manninen, H. E., McMeeking, G., Merikanto, J., Minikin, A., Mirme, S., Morgan, W. T., Nemitz, E., O'Donnell, D., Panwar, T. S., Pawlowska, H., Petzold, A., Pienaar, J. J., Pio, C., Plass-Duelmer, C., Prevot, A. S. H., Pryor, S., Reddington, C. L., Roberts, G., Rosenfeld, D., Schwarz, J., Seland, O., Sellegri, K., Shen, X. J., Shiraiwa, M., Siebert, H., Sierau, B., Simpson, D., Sun, J. Y., Topping, D., Tunved, P., Vaattovaara, P., Vakkari, V., Veeffkind, J. P., Visschedijk, A., Vuollekoski, H., Vuolo, R., Wehner, B., Wildt, J., Woodward, S., Worsnop, D. R., van Zadelhoff, G. -, Zardini, A. A., Zhang, K., van Zyl, P. G., Kerminen, V. -, Carslaw, K. S. and Pandis, S. N.: General overview: European Integrated project on Aerosol Cloud Climate and Air Quality interactions (EUCAARI) - integrating aerosol research from nano to global scales, *Atmos. Chem. Phys.*, **11**, 13061-13143, 10.5194/acp-11-13061-2011, 2011.
- 20 Kulmala, M., Kontkanen, J., Junninen, H., Lehtipalo, K., Manninen, H. E., Nieminen, T., Petaja, T., Sipila, M., Schobesberger, S., Rantala, P., Franchin, A., Jokinen, T., Jarvinen, E., Aijala, M., Kangasluoma, J., Hakala, J., Aalto, P. P., Paasonen, P., Mikkila, J., Vanhanen, J., Aalto, J., Hakola, H., Makkonen, U., Ruuskanen, T., Mauldin, R. L., 3rd, Duplissy, J., Vehkamaki, H., Back, J., Kortelainen, A., Riipinen, I., Kurten, T., Johnston, M. V., Smith, J. N., Ehn, M., Mentel, T. F., Lehtinen, K. E., Laaksonen, A., Kerminen, V. M. and Worsnop, D. R.: Direct observations of atmospheric aerosol nucleation, *Science*, **339**, 943-946, 10.1126/science.1227385 [doi], 2013.
- Kulmala, M., Petaja, T., Ehn, M., Thornton, J., Sipila, M., Worsnop, D. R. and Kerminen, V. -: Chemistry of Atmospheric Nucleation: On the Recent Advances on Precursor Characterization and Atmospheric Cluster Composition in Connection with Atmospheric New Particle Formation, *Annual Review of Physical Chemistry*, Vol 65, **65**, 21-37, 10.1146/annurev-physchem-040412-110014, 2014.
- 30 Kulmala, M., Vehkamaki, H., Petaja, T., Dal Maso, M., Lauri, A., Kerminen, V. M., Birmili, W. and McMurry, P. H.: Formation and growth rates of ultrafine atmospheric particles: a review of observations, *J. Aerosol Sci.*, **35**, 143-176, 10.1016/j.jaerosci.2003.10.003, 2004.
- Kulmala, M., Petaja, T., Nieminen, T., Sipila, M., Manninen, H. E., Lehtipalo, K., Dal Maso, M., Aalto, P. P., Junninen, H., Paasonen, P., Riipinen, I., Lehtinen, K. E. J., Laaksonen, A. and Kerminen, V.: Measurement of the nucleation of atmospheric aerosol particles, *Nat. Protoc.*, **7**, 1651-1667, 10.1038/nprot.2012.091, 2012.
- 35 Laakso, L., Gronholm, T., Kulmala, L., Haapanala, S., Hirsikko, A., Lovejoy, E. R., Kazil, J., Kurten, T., Boy, M., Nilsson, E. D., Sogachev, A., Riipinen, I., Stratmann, F. and Kulmala, M.: Hot-air balloon as a platform for boundary layer profile measurements during particle formation, *Boreal Environ. Res.*, **12**, 279-294, 2007.
- Li, Z., Zhao, X., Kahn, R., Mishchenko, M., Remer, L., Lee, K., Wang, M., Laszlo, I., Nakajima, T. and Maring, H.: 40 Uncertainties in satellite remote sensing of aerosols and impact on monitoring its long-term trend: a review and perspective, in: *Annales Geophysicae*, 2009.



- McNaughton, C. S., Clarke, A. D., Howell, S. G., Pinkerton, M., Anderson, B., Thornhill, L., Hudgins, C., Winstead, E., Dibb, J. E., Scheuer, E. and Maring, H.: Results from the DC-8 Inlet Characterization Experiment (DICE): Airborne versus surface sampling of mineral dust and sea salt aerosols, *Aerosol. Sci. Technol.*, 41, 136-159, 10.1080/02786820601118406, 2007.
- Merikanto, J., Spracklen, D., Mann, G., Pickering, S. and Carslaw, K.: Impact of nucleation on global CCN, *Atmospheric Chemistry and Physics*, 9, 8601-8616, 2009.
- Mirme, S., Mirme, A., Minikin, A., Petzold, A., Horrak, U., Kerminen, V. and Kulmala, M.: Atmospheric sub-3 nm particles at high altitudes, *Atmospheric Chemistry and Physics*, 10, 437-451, 2010.
- Nieminen, T., Yli-Juuti, T., Manninen, H., Petäjä, T., Kerminen, V. and Kulmala, M.: Technical Note: New particle formation event forecasts during PEGASOS-Zeppelin Northern mission 2013 in Hyytiälä, Finland, *Atmospheric Chemistry and Physics Discussions*, 15, 2459-2485, 2015.
- Nieminen, T., Asmi, A., Dal Maso, M., Aalto, P. P., Keronen, P., Petaja, T., Kulmala, M. and Kerminen, V.: Trends in atmospheric new-particle formation: 16 years of observations in a boreal-forest environment, *Boreal Environ. Res.*, 19, SS191-SS191, 2014.
- Nilsson, E., Rannik, Ü, Kulmala, M., Buzorius, G. and O'dowd, C.: Effects of continental boundary layer evolution, convection, turbulence and entrainment, on aerosol formation, *Tellus B*, 53, 441-461, 2001.
- O'Dowd, C., Yoon, Y., Junkerman, W., Aalto, P., Kulmala, M., Lihavainen, H. and Viisanen, Y.: Airborne measurements of nucleation mode particles I: coastal nucleation and growth rates, *Atmospheric Chemistry and Physics*, 7, 1491-1501, 2007.
- O'Dowd, C., Yoon, Y., Junkermann, W., Aalto, P., Kulmala, M., Lihavainen, H. and Viisanen, Y.: Airborne measurements of nucleation mode particles II: boreal forest nucleation events, *Atmospheric Chemistry and Physics*, 9, 937-944, 2009.
- Paris, J., Arshinov, M. Y., Ciais, P., Belan, B. D. and Nédélec, P.: Large-scale aircraft observations of ultra-fine and fine particle concentrations in the remote Siberian troposphere: New particle formation studies, *Atmos. Environ.*, 43, 1302-1309, 2009.
- Petäjä, T., O'Connor, E. J., Moisseev, D., Sinclair, V. A., Manninen, A. J., Väänänen, R., von Lerber, A., Thornton, J. A., Nicoll, K., Petersen, W., Chandrasekar, V., Smith, J. N., Winkler, P. M., Krüger, O., Hakola, H., Timonen, H., Brus, D., Laurila, T., Asmi, E., Riekkola, M., Mona, L., Massoli, P., Engelmann, R., Komppula, M., Wang, J., Kuang, C., Bäck, J., Virtanen, A., Levula, J., Ritsche, M. and Hickmon, N.: BAEECC A field campaign to elucidate the impact of Biogenic Aerosols on Clouds and Climate, *Bull. Amer. Meteor. Soc.*, 10.1175/BAMS-D-14-00199.1, 2016.
- Petzold, A., Thouret, V., Gerbig, C., Zahn, A., Brenninkmeijer, C., Gallagher, M., Hermann, M., Pontaud, M., Ziereis, H., Boulanger, D., Marshall, J., Nédélec, P., Smit, H., Friess, U., Flaud, J., Wahner, A., Cammas, J. and Volz-Thomas, A.: Global-scale atmosphere monitoring by in-service aircraft - current achievements and future prospects of the European Research Infrastructure IAGOS, *Tellus B*, 67, 2015.
- Petzold, A., Rasp, K., Weinzierl, B., Esselborn, M., Hamburger, T., Doernbrack, A., Kandler, K., Schuetz, L., Knippertz, P., Fiebig, M. and Virkkula, A.: Saharan dust absorption and refractive index from aircraft-based observations during SAMUM 2006, *Tellus Ser. B-Chem. Phys. Meteorol.*, 61, 118-130, 10.1111/j.1600-0889.2008.00383.x, 2009.



- Rolph, G. D.: Real-time Environmental Applications and Display sYstem (READY) Website (<http://www.ready.noaa.gov>), NOAA Air Resources Laboratory, College Park, MD, 2016.
- Rose, C., Sellegri, K., Freney, E., Dupuy, R., Colomb, A., Pichon, J., Ribeiro, M., Bourianne, T., Burnet, F. and Schwarzenboeck, A.: Airborne measurements of new particle formation in the free troposphere above the Mediterranean Sea during the HYMEX campaign, *Atmospheric Chemistry and Physics*, 15, 10203-10218, 2015.
- Schobesberger, S., Vaananen, R., Leino, K., Virkkula, A., Backman, J., Pohja, T., Siivola, E., Franchin, A., Mikkila, J., Paramonov, M., Aalto, P. P., Krejci, R., Petaja, T. and Kulmala, M.: Airborne measurements over the boreal forest of southern Finland during new particle formation events in 2009 and 2010, *Boreal Environ. Res.*, 18, 145-163, 2013.
- Sheridan, P., Andrews, E., Ogren, J., Tackett, J. and Winker, D.: Vertical profiles of aerosol optical properties over central Illinois and comparison with surface and satellite measurements, *Atmospheric Chemistry and Physics Discussions*, 12, 17187-17244, 2012.
- Sogacheva, L., Dal Maso, M., Kerminen, V. - and Kulmala, M.: Probability of nucleation events and aerosol particle concentration in different air mass types arriving at Hyytiälä, southern Finland, based on back trajectories analysis., *Boreal Env. Res.*, 10, 479-491, 2005.
- Spracklen, D. V., Carslaw, K. S., Kulmala, M., Kerminen, V., Sihto, S., Riipinen, I., Merikanto, J., Mann, G. W., Chipperfield, M. P., Wiedensohler, A., Birmili, W. and Lihavainen, H.: Contribution of particle formation to global cloud condensation nuclei concentrations, *Geophys. Res. Lett.*, 35, n/a-n/a, 10.1029/2007GL033038, 2008.
- Stein, A., Draxler, R., Rolph, G., Stunder, B., Cohen, M. and Ngan, F.: NOAA's HYSPLIT atmospheric transport and dispersion modeling system, *Bull. Am. Meteorol. Soc.*, 96, 2059-2077, 2015.
- Stull, R. B.: *An introduction to boundary layer meteorology*, Springer Science & Business Media, 2012.
- Vanhanen, J., Mikkilä, J., Lehtipalo, K., Sipilä, M., Manninen, H., Siivola, E., Petäjä, T. and Kulmala, M.: Particle size magnifier for nano-CN detection, *Aerosol Science and Technology*, 45, 533-542, 2011.
- Wehner, B., Siebert, H., Ansmann, A., Ditas, F., Seifert, P., Stratmann, F., Wiedensohler, A., Apituley, A., Shaw, R. and Manninen, H. E.: Observations of turbulence-induced new particle formation in the residual layer, *Atmospheric chemistry and physics*, 10, 4319-4330, 2010.
- Wehner, B., Siebert, H., Stratmann, F., Tuch, T., Wiedensohler, A., Petäjä, T., Dal Maso, M. and Kulmala, M.: Horizontal homogeneity and vertical extent of new particle formation events, *Tellus B*, 59, 362-371, 2007.
- Williams, J., Crowley, J., Fischer, H., Harder, H., Martinez, M., Petäjä, T., Rinne, J., Bäck, J., Boy, M., Dal Maso, M., Hakala, J., Kajos, M., Keronen, P., Rantala, P., Aalto, J., Aaltonen, H., Paatero, J., Vesala, T., Hakola, H., Levula, J., Pohja, T., Herrmann, F., Auld, J., Mesarchaki, E., Song, W., Yassaa, N., Nölscher, A., Johnson, A. M., Custer, T., Sinha, V., Thieser, J., Pouvesle, N., Taraborrelli, D., Tang, M. J., Bozem, H., Hosaynali-Beygi, Z., Axinte, R., Oswald, R., Novelli, A., Kubistin, D., Hens, K., Javed, U., Trawny, K., Breitenberger, C., Hidalgo, P. J., Ebben, C. J., Geiger, F. M., Corrigan, A. L., Russell, L. M., Ouwersloot, H. G., Vila-Guerau de Arellano, J., Ganzeveld, L., Vogel, A., Beck, M., Bayerle, A., Kampf, C. J., Bertelmann, M., Köllner, F., Hoffmann, T., Valverde, J., Gonzalez, D., Riekkola, M. -, Kulmala, M. and Lelieveld, J.: The summertime Boreal forest field measurement intensive (HUMPPA-COPEC-2010): an overview of meteorological and chemical influences, *Atmospheric Chemistry and Physics*, 11, 10599-10618, 2011.



Zhang, R., Khalizov, A., Wang, L., Hu, M. and Xu, W.: Nucleation and Growth of Nanoparticles in the Atmosphere, Chem. Rev., 112, 1957-2011, 10.1021/cr2001756, 2012.

## 5 Tables

**Table 1. List of used airborne particle and gas instruments**

Instrument	Quantity	Range
Ultrafine condensation particle counter TSI 3776 (uCPC)	Particle number concentration	>3 nm
Scanning mobility particle sizer (SMPS)	Particle size distributions	10–400 nm
Li-Cor Li-840	CO <sub>2</sub> / H <sub>2</sub> O concentration	CO <sub>2</sub> 0–20,000 ppm H <sub>2</sub> O 0–60 ppt

**Table 2. Characteristic numbers of the case study flights**

Date	Flight time around Hyytiälä	NPF observed at Hyytiälä	Temperature on ground	Wind on ground	Origin of air mass	PBL height	Clouds
28.3.2014	10:05–12:15	10:50	6–8 °C	1 m/s, E	Arctic Ocean	700–1180 m	0/8
	14:35–16:20		11–9 °C	1 m/s, NW		1040–1070 m	0/8
16.5.2013	8:20–10:40	09:07	17–18 °C	2 m/s, SE	West-Europe, Atlantic Ocean	740–1450 m	0/8
	14:05–16:10		20 °C	2m/s, SE		1860–1920 m	0/8
26.3.2014	10:25–12:25	10:40	6–8 °C	2 ms, NE	Northwards, Atlantic Ocean	670–840 m	0/8
26.3.2014	15:10–17:10		10–4 °C	2m/s, NE		860–890 m	0/8
4.4.2014	3:40–5:10		-5 – -6 °C	1 m/s NW	North, Arctic Ocean	-	0/8–7/8



**Table 3: Class I NPF event days. Comparison of particle concentration and diameter between Hyytiälä station and aircraft-borne measurements inside the PBL. Median values of the relative difference of the total number concentration ( $N_{\text{tot}}$ ), concentration of particles with diameter 10–25 nm ( $N_{10-25}$ ) and 80–400 nm ( $N_{80-400}$ ) are presented.  $D_p$  (<25 nm) difference of the airborne and ground-based mode peak diameter of sub-25 nm mode. See absolute ranges in supplementary Table S2.**

Flight	Date	$N_{\text{tot}}$ $\Delta$ , %	$N_{10-25}$ $\Delta$ , %	$N_{80-400}$ $\Delta$ , %	$D_p$ (<25 nm) $\Delta$ , nm
2013_8	8.5.2013	34	44	1	2 nm
2013_9	8.5.2013	25	53	-1	-
2013_15	15.5.2013	17	21	6	-3 nm
2013_45	15.6.2013	27	44	11	-2 nm
<b>Median all flights 2013</b>		<b>9 %</b>	<b>32 %</b>	<b>0.5 %</b>	<b>-7 nm</b>
2014_4	26.3.2014	99	83	9	-2 nm
2014_5	26.3.2014	29	54	-35	-2 nm
2014_6	27.3.2014	44	92	6	31 nm
2014_7	27.3.2014	7	65	-3	-2 nm
2014_8	28.3.2014	73	63	10	-2 nm
2014_9	28.3.2014	37	71	41	-1 nm
2014_10	31.3.2014	36	76	16	2 nm
2014_11	31.3.2014	11	27	2	12 nm
2014_19	4.4.2014	56	50	5	-1 nm
2014_21	8.4.2014	25	25	-2	0 nm
2014_22	8.4.2014	-1	26	3	-2 nm
2014_23	9.4.2014	39	66	2	-2 nm
2014_24	9.4.2014	16	57	0	0 nm
2014_25	10.4.2014	56	56	10	20 nm
2014_26	10.4.2014	81	86	1	-2 nm
<b>Median all flights 2014</b>		<b>11 %</b>	<b>57 %</b>	<b>1 %</b>	<b>-3 nm</b>



5

**Table 4.** Cases when small particles ( $\sim < 25$  nm) were detected above the PBL. Time shows the approximated passing time of the layer, or the time period when the layer was observable if the flight consisted of more than one climb. Diameter is the mode peak diameter of the nucleation mode from the mode fitting calculations. When there is (\*) in the total concentration column, the concentration of the layer was not higher than the concentration in the surrounding altitudes, only the shape of the distribution was different. Column ‘cloud’ indicates when there has been clouds along the back trajectory during the previous 12–24 hours. Column ‘Lifting from PBL’ shows how many hours before the air mass has been connected to the PBL according to the 96-h backward trajectories

Flight no	Date	Time	Altitude (m a.s.l.)	Diameter (nm)	Total conc. ( $\text{cm}^{-3}$ )	Clouds	Lifting from PBL
2013_5	6.5.2013	9:00–10:00	2000m->	20 nm		20 h	20 h
2013_11	11.5.2013	15:30	2500 m	15 nm	1600 (*)	15 h	-
2013_13	14.5.2013	11:00	2200–2700 m	20–30 nm	2000–3000	-	-
2013_14	15.5.2013	10:00–11:00	2500–2800 m	7–15 nm	3000–5000	16 h	16 h
2013_23	23.5.2013	9:30	2600 m	17 nm	1000	12 h	-
2013_26	26.5.2013	13:30	3000 m	11 nm	1000 (*)	24 h	36 h
2013_28	28.5.2013	10:30	2500–3000 m	27 nm	2000–4000	12h	72 h
2013_29	29.5.2013	11:30	2500–3000 m	11–16 nm	1500 (*)	20 h	32 h
2013_39	8.6.2013	22:00	2500–3000 m	25 nm	1200 (*)	-	24 h
2014_4	26.3.2014	11:00–12:00	2000–2800 m	<10 nm	2000–3000	24 h	60 h
2014_5		16:00	1800–2400 m	<10–10 nm	2800		
2014_6	27.3.2014	12:00	2800–3800	<10 nm	2000–3000	15 h	48 h
2014_7		16:00	2500–2800 m	10–15 nm	2000–4000		
2014_8	28.3.2014	10:45–11:15	2700–3000 m	<10 nm	200 (*)	12 h	48 h
2014_11	31.3.2014	13:30	2000 m	15 nm	500	12 h	18 h
2014_14	2.4.2014	10:00–11:00	2500–2800 m	10–15 nm	1000–1500	13 h	-
2014_15		15:30	2300 m	15–20 nm	600–900		
2014_19	4.4.2014	10:20	1900–2600 m	<10 nm	1200–4500	22 h	-
2014_21	8.4.2014	10:00	2500 m	<10 nm	1000	15 h	48 h
2014_22		16:00	2500 m	25 nm	800–900		



## Figures



**Figure 1.** Upper left panel: The instrumented Cessna 172 aircraft. Down left panel: The sample air inlet under the wing, and an aerial view towards Hyytiälä measurement station. Right panel: Measurement instruments on-board.

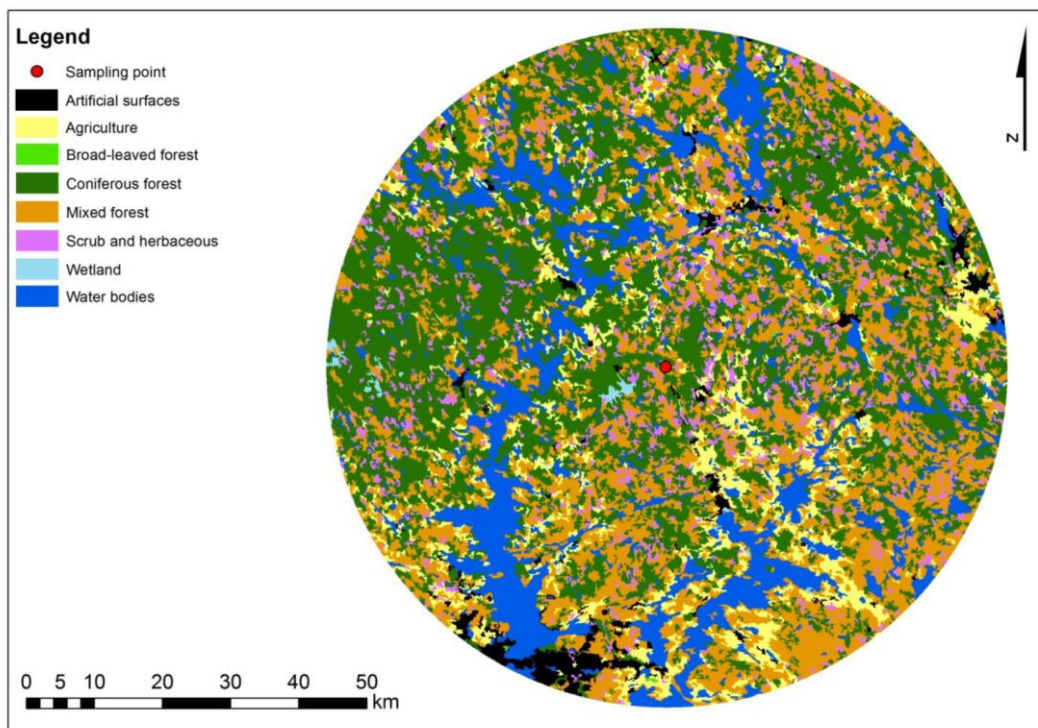
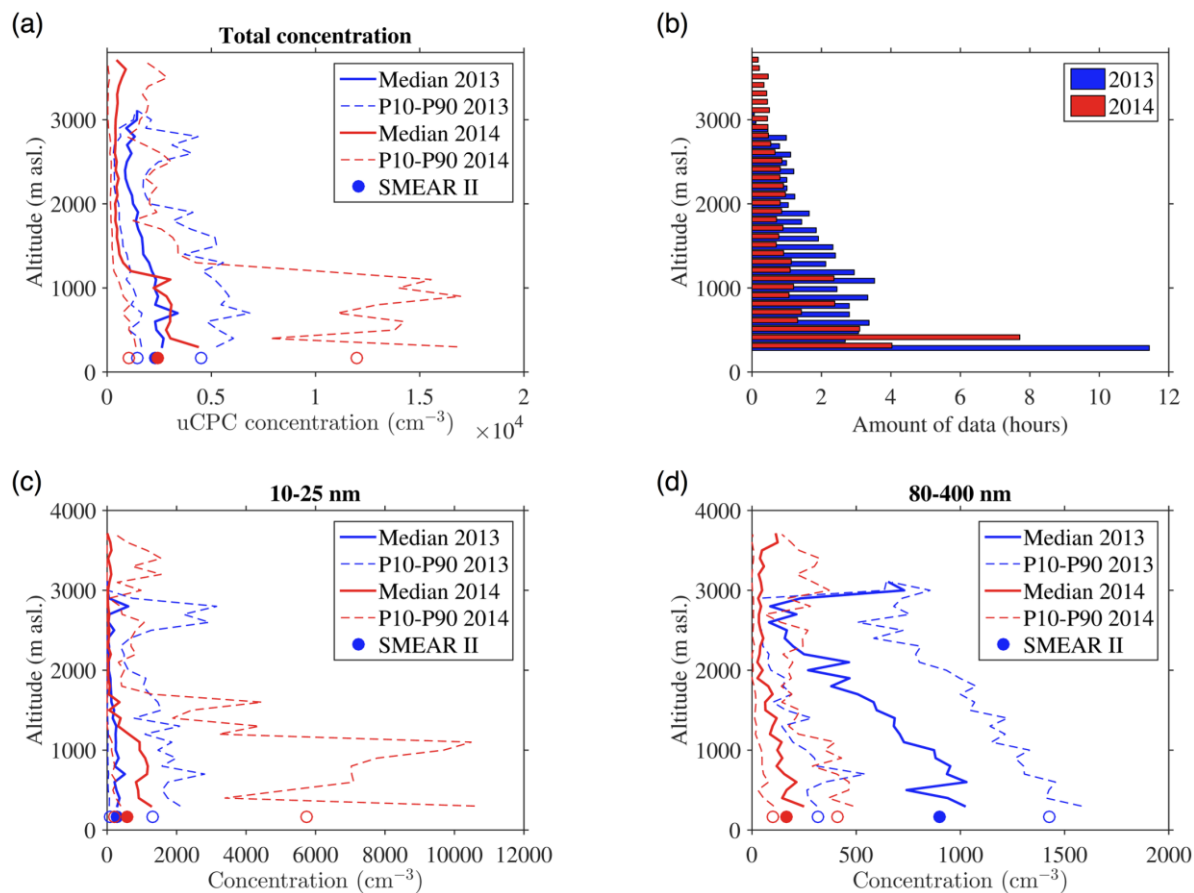
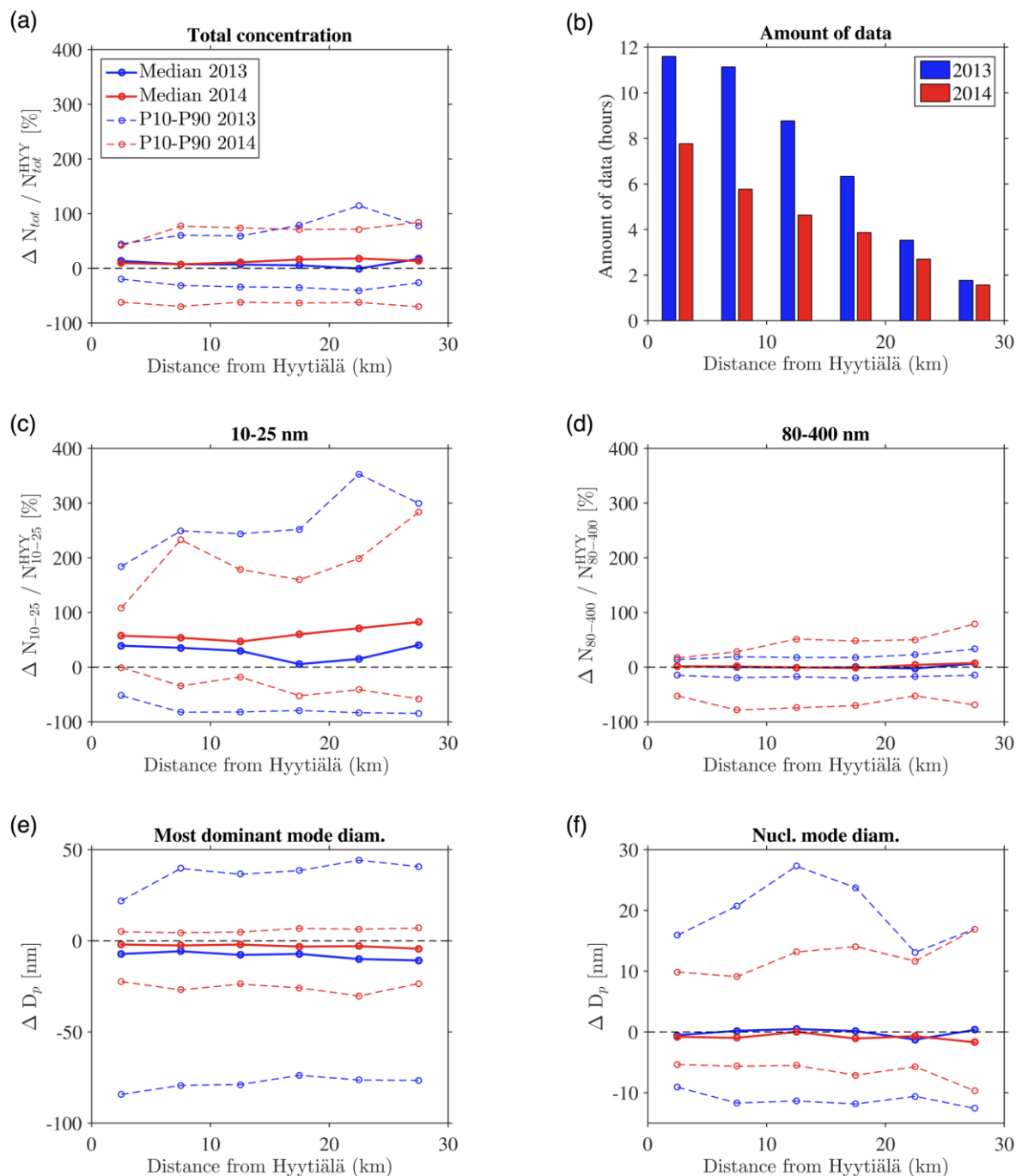


**Figure 2.** The land use map of Hyytiälä area. The red dot in the middle of the figure refers to Hyytiälä, and the large black area in the SW is Tampere city. (EEA 1997, Williams et al. 2011)



5 **Figure 3.** Statistical vertical particle number concentration profiles calculated separately for all data of late spring flights 2013 (blue), and early spring flights 2014 (red). Total concentration (a), and concentrations of 10–25 nm (c) and 80–400 nm (d) plotted separately. Altitude axis is divided to 100 m bins. Panel b) shows the relative amount of data inside each bin. Panels (a,c,d) shows the median, 10th, and 90th percentile concentration profiles measured in Hyytiälä area. Circles show the median (solid circles), 10th, and 90th percentiles (open circles) calculated from simultaneous Hyytiälä data.



5 **Figure 4.** Variability between Cessna and Hyttiälä measurements in concentration and diameter as a function of distance from Hyttiälä. The panel a) shows the percentiles of relative difference in total concentration. The median relative difference in concentration measured at Cessna compared to the concentration measured at Hyttiälä, in %. P10 and P90 are the 10<sup>th</sup> and 90<sup>th</sup> percentiles of the same relative difference. Positive values refer that the concentration measured with Cessna is higher. Panel b) is



**the amount of data inside each distance bin. Statistics weakens when the distance grows. Panel c) and d) show the distribution of the relative difference for concentration of particles with diameter of 10–25 nm and 80–400 nm, respectively. In panel e) is the absolute difference in diameter (nm) of the simultaneous modes with highest concentration, in panel f) the absolute difference in diameter of the smallest mode when there is a <25 nm mode in Hyttiälä.**



28 March 2014 Morning flight

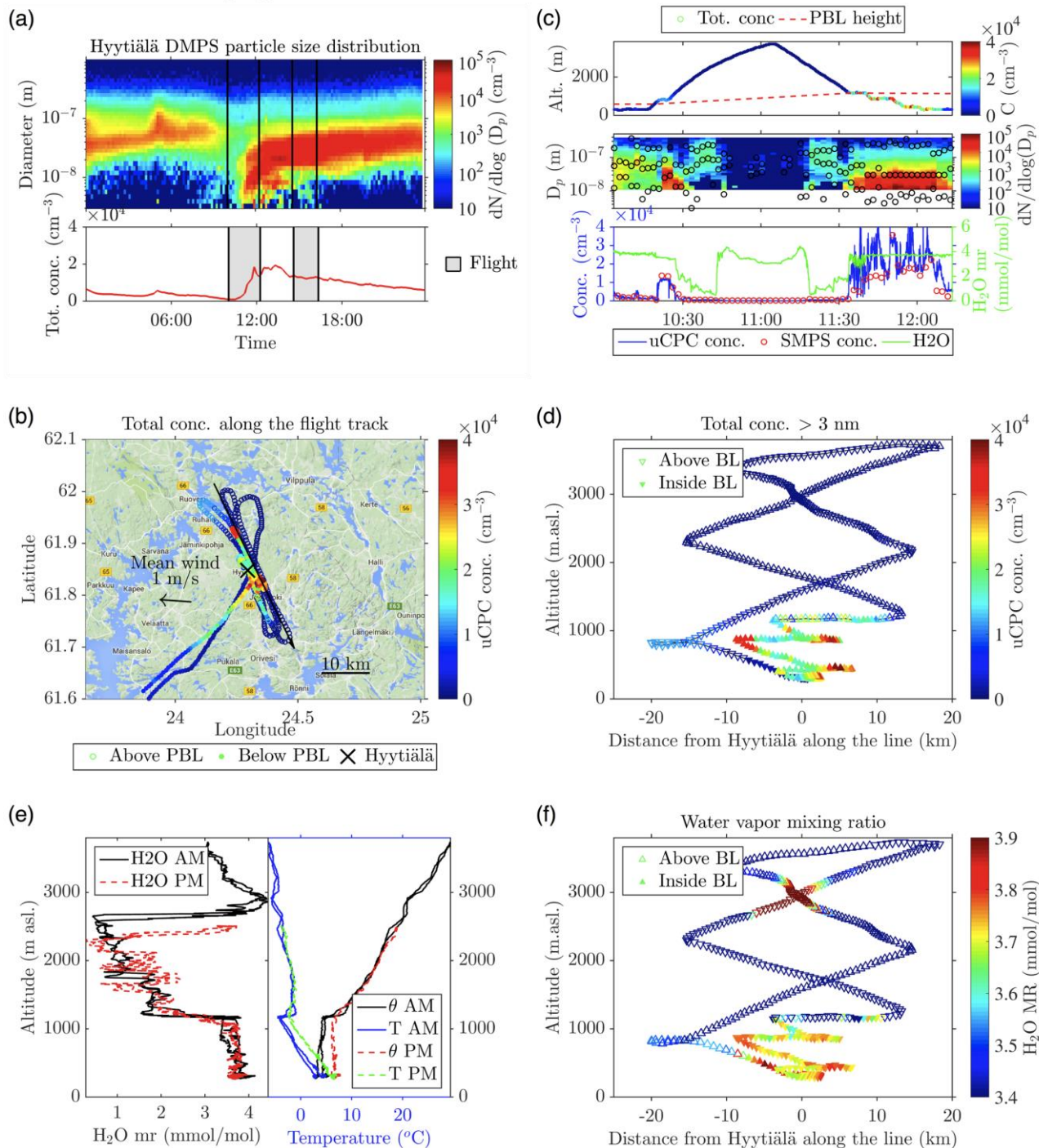
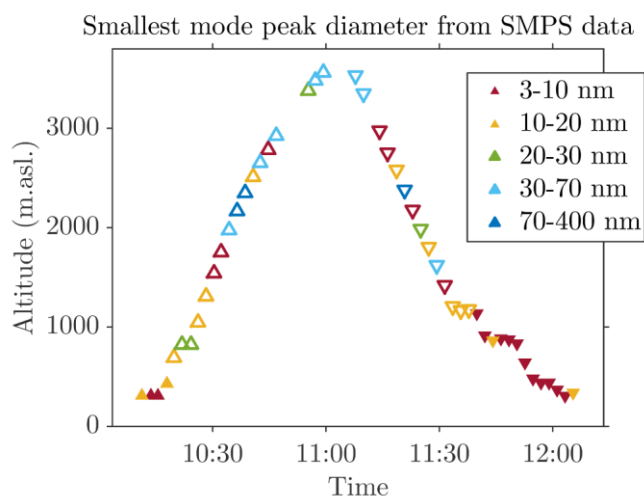


Figure 5. Observed particle concentration and size distribution at and around Hyttiälä measurement station during the first flight on 28 March 2014. Panel a) is the Hyttiälä DMPS number size distribution during that day. The flight times are marked with gray



5 areas. Panel b) shows the flight track with the total number concentration as a color. Time series in panel c) show the 1) flying altitude and the number concentration together with the PBL height, 2) the number size distribution and 3) total number concentration measured with ultrafine CPC (>3 nm) and SMPS (10–400 nm) together with the H<sub>2</sub>O MR along the flight. In panels d) and f) we have projected the flight track to a line in xy-space (arrow in the panel b) and plotted the altitude against the distance from Hyytiälä along this line. The color shows the total number concentration (>3 nm) and H<sub>2</sub>O MR along the flight track. In panel e) is plotted the H<sub>2</sub>O MR, temperature and potential temperature ( $\theta$ ) as a function of the altitude during both AM and PM flights.





### 28 March 2014 Afternoon flight

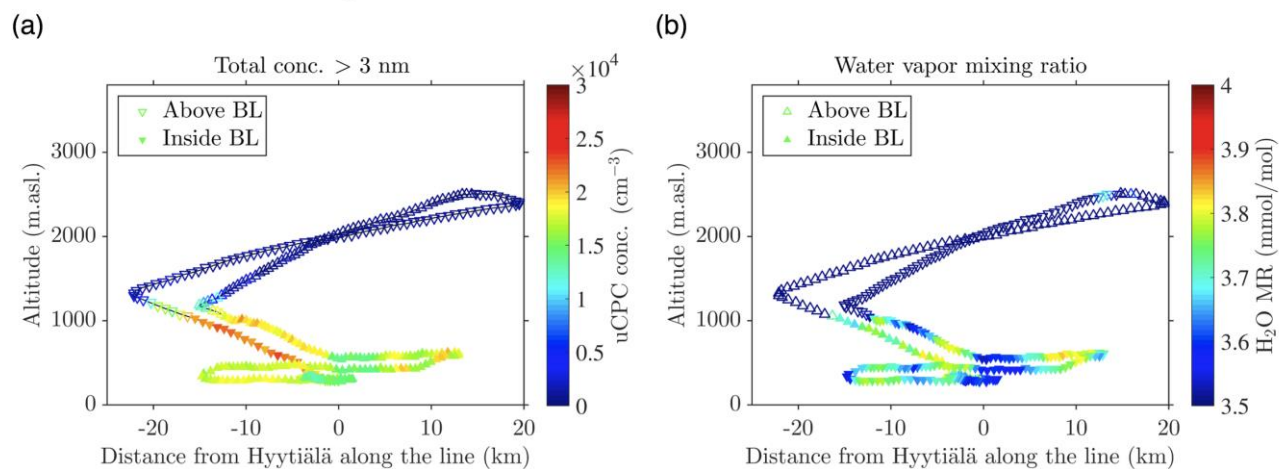
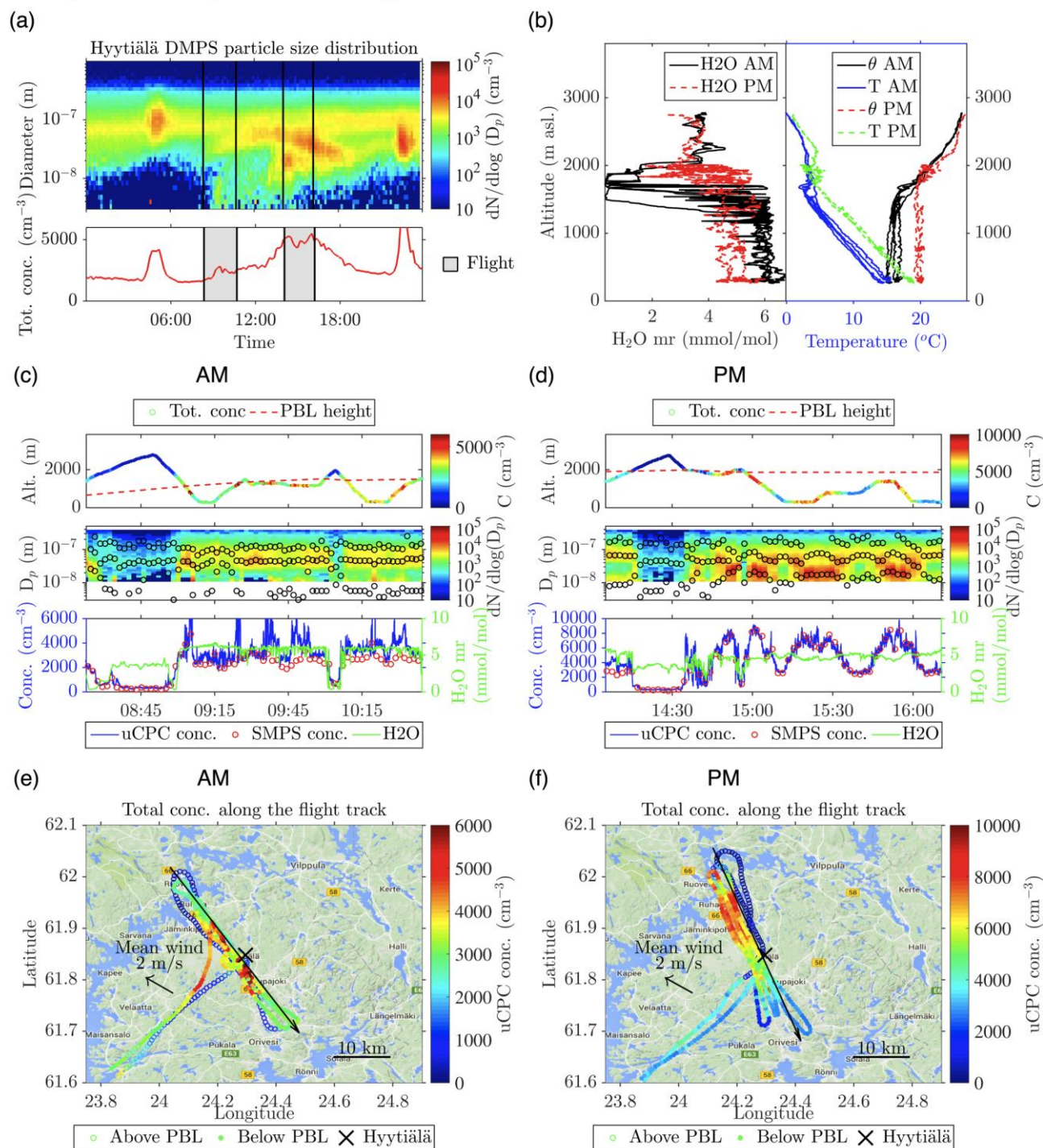


**Figure 7. Observed particle number concentration and H<sub>2</sub>O MR around Hyytiälä measurement station at different altitudes during the second flight on 28 March 2014. The flight track had almost same orientation as at morning, and thus the direction of the x-axis is from NW to SE.**



16 May 2013 Morning and afternoon flights





5 **Figure 8. Observed particle concentration and size distribution at and around Hyttiälä measurement station during two flights on 16 May 2013. Panel a) shows the aerosol size distribution time series in Hyttiälä, and panel b) shows the measured H<sub>2</sub>O MR, potential temperature ( $\theta$ ) and temperature profiles during the morning and afternoon flights. Left panels (c and e) are from morning flight and right ones (d and f) from afternoon flight. See Fig. 5 for caption of panel c). Panels e) and f) show the particle number concentration on a map. See Fig. 9 for quantities projected along the lines shown in the maps.**



### 16 May 2013 Morning and afternoon flights

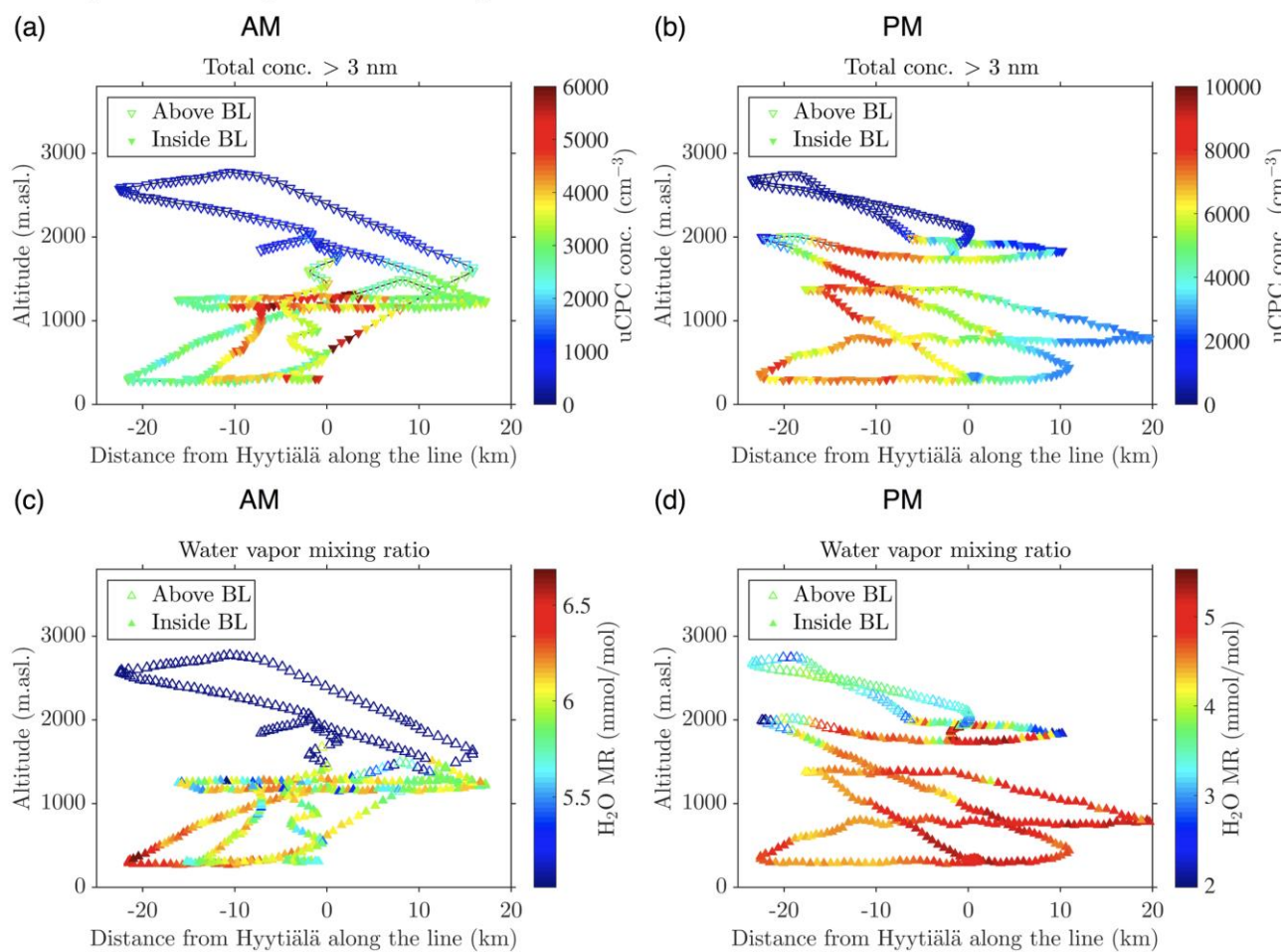
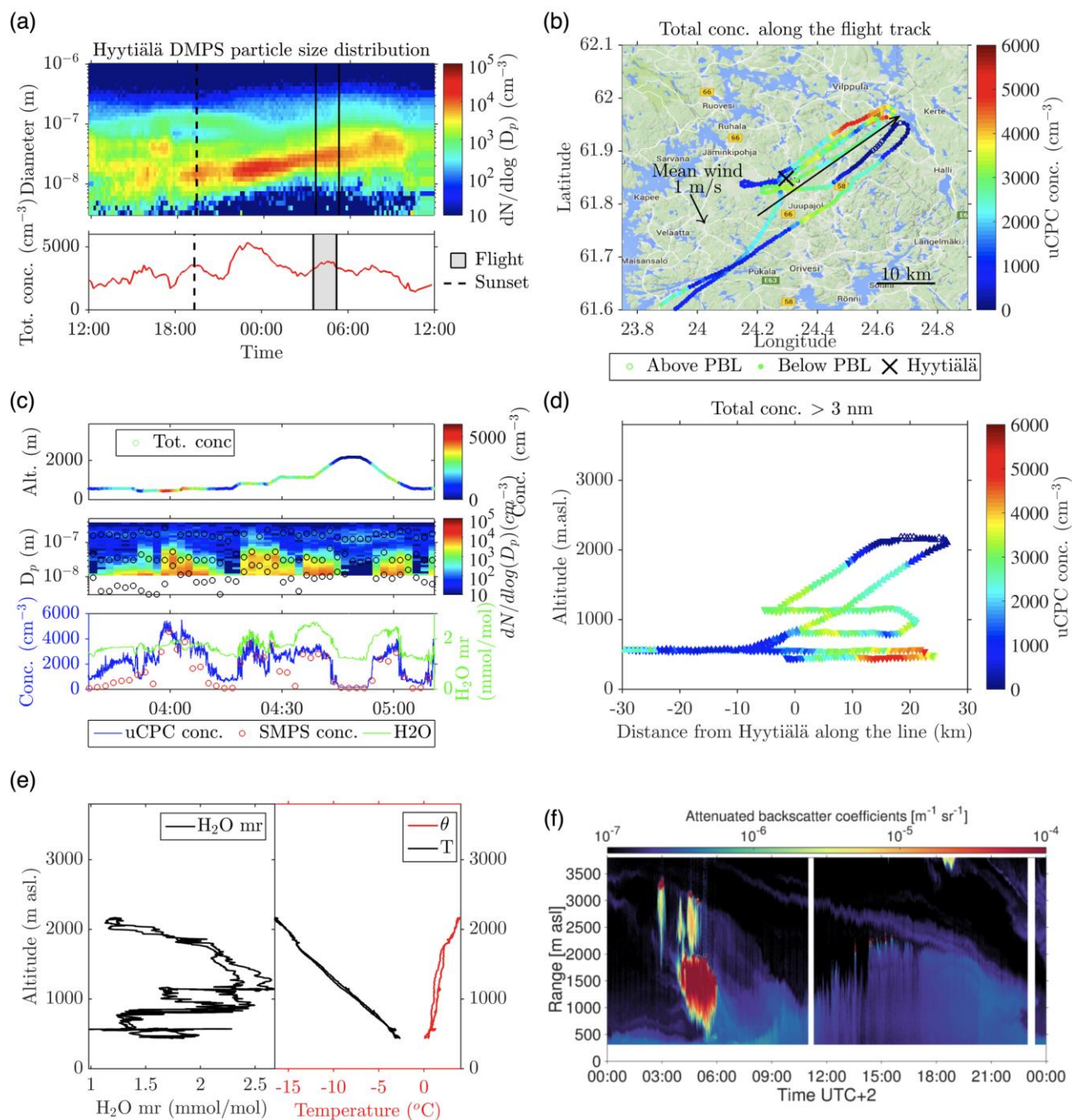


Figure 9. Observed particle concentration (a-b) and H<sub>2</sub>O MR (c-d) projected along a line shown in maps Figs. 8e and f.



4 April 2014, early hours flight





5 **Figure 10.** Observed particle concentration and size distribution at and around Hyttiälä measurement station during a flight on 4 April 2014. Panel a) is the Hyttiälä DMPS number size distribution between 3 April at 12:00 and 4 April at 12:00. The flight times are marked with gray areas. A dotted black line marks the sunset at 19:16. Panel b) shows the flight track and the color is the total number concentration. See Fig. 5 for caption of panel c). In panels d) we have projected the flight track to a line in xy-space (arrow in the panel b) and plotted the altitude against the distance from Hyttiälä along this line. The color shows the total number concentration (>3 nm). In panel e) is plotted the H<sub>2</sub>O MR, temperature and potential temperature as a function of the altitude. Panel e) shows the HSRL lidar data where the narrow vertical lines mark flight times, whereas the wider vertical gaps correspond to missing profiles.

10

### 26 March 2014 Morning and afternoon flights

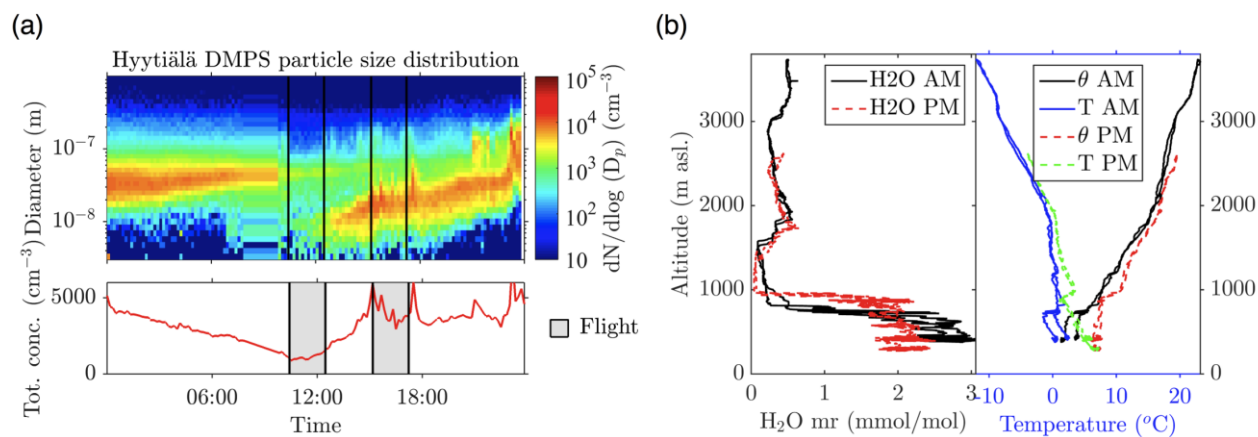
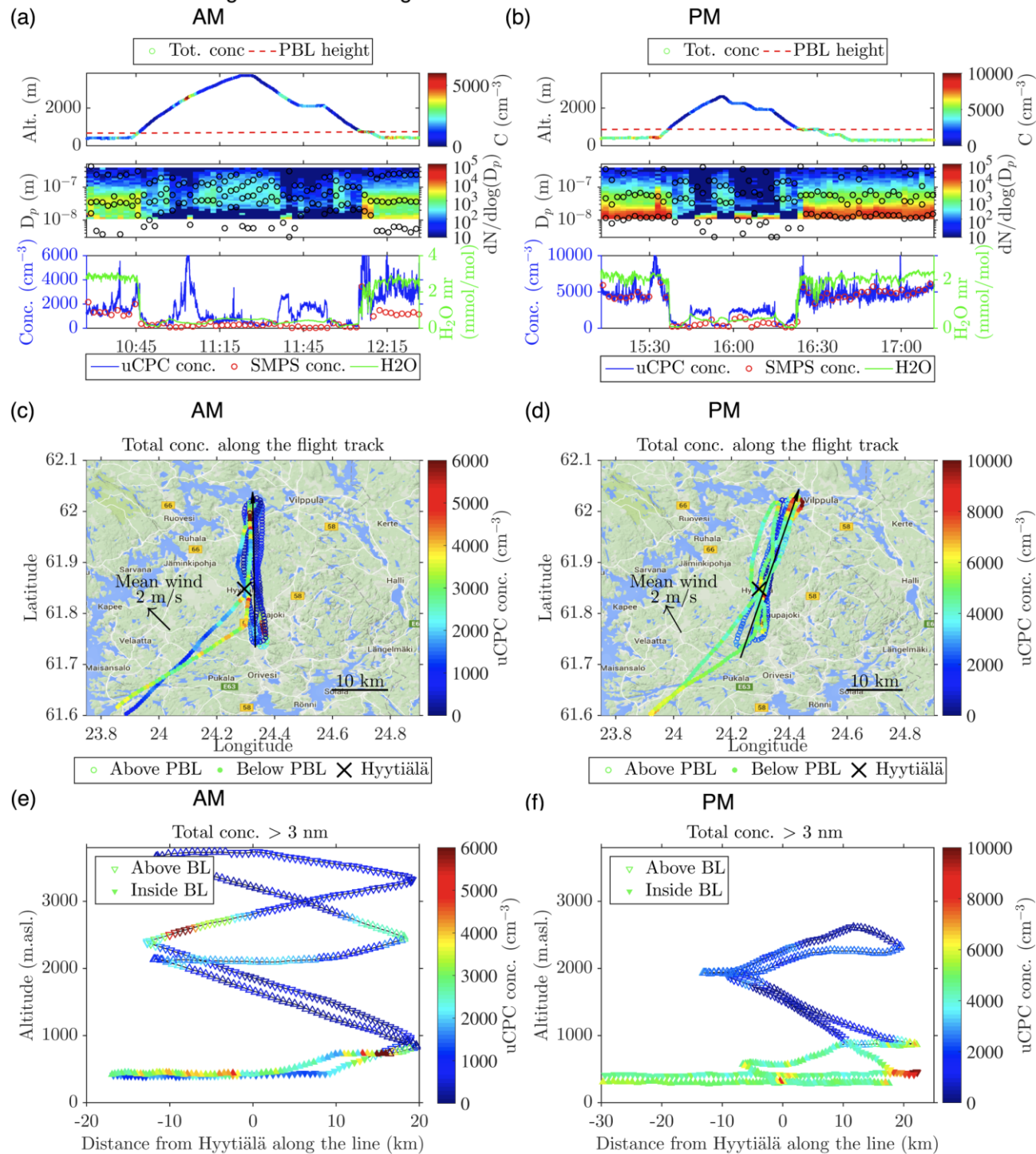


**Figure 11.** Observed particle concentration and size distribution at Hyttiälä on 26 March 2014. Panel a) shows the Hyttiälä DMPS size distribution, the flight times are marked with gray areas. In panel b) are presented the measured vertical H<sub>2</sub>O MR, potential temperature (θ) and temperature profiles during the morning and afternoon flights.

15



26 March 2014 Morning and afternoon flights





5 **Figure 12. Observed particle concentration and size distribution at and around Hyytiälä measurement station during two flights on 26 March 2014. Left panels are from morning flight and right ones from afternoon flight. See Fig. 5 for captions of panels a and b). Panels c) and d) show the particle number concentration on a map, and in panels e) and f) we have projected the flight tracks to lines in xy-space (arrow in the panel c and d) ) and plotted the altitude against the distance from Hyytiälä along this line. The color shows the total number concentration along the flight track.**

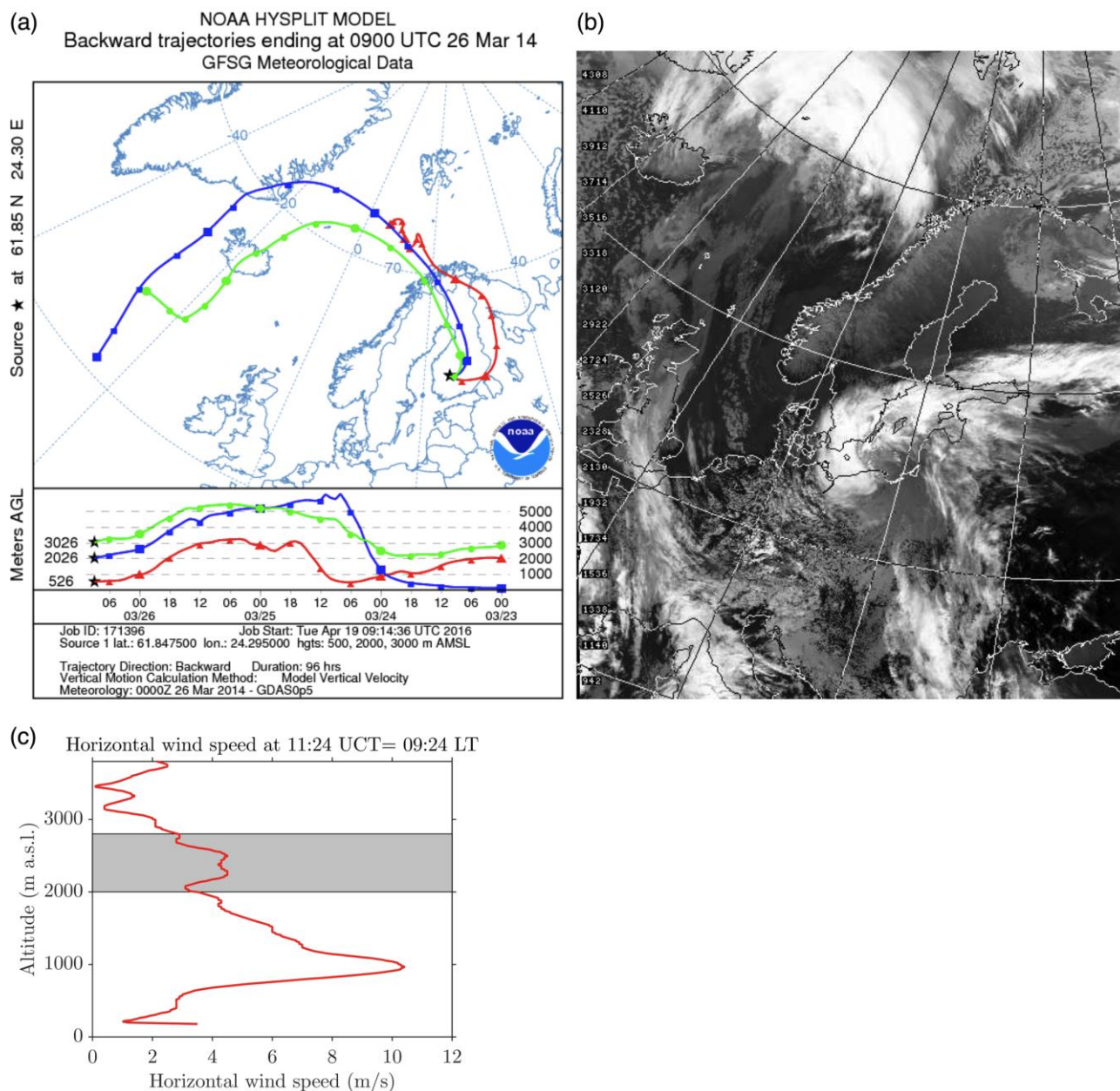


**Figure 13.** Panel a) indicates the origin of the air masses arriving to Hyttiälä 26.3.2014 at 11 local time, and panel b) shows AVHRR satellite image on 25.3.2014 at 11:55 UTC (Thermal infra-red channel, 10.3–11.3µm) © NERC Satellite Receiving Station, Dundee University, Scotland (<http://www.sat.dundee.ac.uk>). Panel c) shows the horizontal wind profile.